

QATAR UNIVERSITY  
COLLEGE OF ENGINEERING  
MECHANICAL RESPONSE OF APPLYING DIFFERENT PARAMETERS ON  
NEGATIVE STIFFNESS HONEYCOMB STRUCTURE  
BY  
ABDALLA RABIE TAKROUNY

A Thesis Submitted to  
the College of Engineering  
in Partial Fulfillment of the Requirements for the Degree of  
Master of Science in Mechanical Engineering

January 2023

© 2023 Abdalla Rabie Takrouny. All Rights Reserved.

## COMMITTEE PAGE

The members of the Committee approve the Thesis of  
Abdalla Rabie Takrouny defended on 02/01/2023.

---

Dr. Faris Tarlochan  
Thesis/Dissertation Supervisor

---

Dr. Khurshid Alam  
Committee Member

---

Dr. Shiming Deng  
Committee Member

---

Dr. Nuri Onat  
Committee Member

Approved:

---

Khalid Kamal Naji, Dean, College of Engineering

## ABSTRACT

TAKROUNY, ABDALLA RABIE, Masters: January : [2023],

Masters of Science in Mechanical Engineering

Title: Mechanical Response of Applying Different Parameters on Negative Stiffness Honeycomb Structure

Supervisor of Thesis: Faris Tarlochan.

It has become apparent that negative stiffness behavior may have potential applications in vibration isolation mechanisms, vibro-acoustic dampening materials, and mechanical switches. Unlike traditional honeycombs, due to these properties, a negative honeycomb can absorb substantial amounts of mechanical energy whilst maintaining a stable stress. This thesis investigates the force threshold under displacement loading of three parameters applied on different models of negative-stiffness honeycomb (NSH) structures. The three parameters are material applied on the structure, honeycomb unit cell, and beam thickness of the negative honeycomb structure. Each part of this parameter is divided into three different variables. First, nylon 11, nylon 12 and nylon 6/6 which are widely used as polymer material were applied on the honeycomb model. Then, three different beam thickness of 6.35 mm, 12.7 mm and 19.05 mm were modeled and unit cell of 4, 5 and 7 numbers of arrangement were created using LS-Dyna software. Accordingly, 27 models were developed, and the three varied materials were assigned repeatably to each model and then force threshold were evaluated. The Finite element analysis (FEA) for formed model was validated and shows force value of 289 N with an error of 5% compared to the referenced model. In the 4- unit cell model, the highest force threshold of approximately 240 N was noticed during loading phase at the beam thickness of 19.05 mm for both nylon 11 and 12 material. While for the 5-unit cell honeycomb structure,

the highest value for force was observed (591 N) at largest beam thickness of 19.05 mm. Finally, the force threshold of nearly 550 N during loading and unloading phases was observed for nylon 6/6 material at beam thickness of 19.05 mm that was almost 1.2 times forces required for nylon 11 and 12 during first peak of loading and unloading phase. The results obtained confirm the negative stiffness behavior on the studied models and shows that the force threshold applied is reduced comparing to forces required in the conventional honeycombs models. Thus, it has the potential to be used for impact-sensitive applications such as bicycle seats and food packaging.

## DEDICATION

*This Thesis dedicated to my supportive family and my lovely fiancée. Thank you all for supporting me to finish my thesis. Many thanks to my father for helping me and supporting me through my academic career. Special thanks to my supervisor, Dr. Faris Tarlochan, for being patient with me and supported me to complete my thesis.*

## ACKNOWLEDGMENTS

I would like to acknowledge the support of Qatar University for providing all the needs to complete my thesis study. I am grateful to Dr. Faris Tarlochan for the massive support and his faith on me to provide and support with all provided information to finalize my thesis study. Massive thanks to Eng. Ameen Topa for all information provided that helped me to model and complete all simulation work of my thesis.

## TABLE OF CONTENTS

DEDICATION .....	v
ACKNOWLEDGMENTS .....	vi
LIST OF TABLES .....	ix
LIST OF FIGURES .....	x
Chapter 1: INTRODUCTION.....	1
1.1 Background .....	1
1.2 Problem statement.....	3
1.3 Research objectives .....	4
1.4 Thesis layout .....	4
CHAPTER 2: LITERATURE REVIEW .....	6
2.1 Introduction .....	6
2.2 Prefabrication curved beams and relationships .....	6
2.3 Negative stiffness honeycomb structures .....	11
CHAPTER 3: METHODOLOGY .....	15
3.1 Introduction .....	15
3.2 Finite Element Modeling.....	15
3.2.1 Model geometry.....	16
3.2.2 modeling of material.....	17
3.2.3 Boundary conditions and control.....	18
3.2.4 Validation of the honeycomb model .....	19

3.3 Parametric study for the negative stiffness honeycomb model.....	19
CHAPTER 4: RESULTS & DISSCUSIONS .....	22
4.1 Model Validation.....	22
4.2 Effect of Material Type .....	24
4.3 Effect of Beam width .....	26
4.4 Effect of multiple honeycomb unit-cell structure .....	27
4.5 Results of parametric study .....	29
4.5.1 Result for 4-unit cell of beam thickness 6.35 mm.....	31
4.5.2 Result for 4-unit cell of beam thickness 12.7 mm.....	33
4.5.3 Result for 4-unit cell of beam thickness 19.05 mm.....	34
4.5.4 Result for 5-unit cell of beam thickness 6.35 mm.....	35
4.5.5 Result for 5-unit cell of beam thickness 19.05 mm.....	36
4.5.6 Result for 7-unit cell of beam thickness 6.35 mm.....	37
4.5.7 Result for 7-unit cell of beam thickness 12.7 mm.....	38
4.5.8 Result for 7-unit cell of beam thickness 19.05 mm.....	39
CHAPTER 5: CONCLUSION AND FUTURE WORK.....	40
References.....	45
Appendix I: LS-DYNA Simulation models.....	50
Appendix II: Case study Ls-topology optimization tool.....	52



## LIST OF TABLES

Table 1. Material properties of applied materials on the model. ....	18
Table 2. properties of the selected materials in this study. ....	18
Table 3. Parametric study applied on the honeycomb model. ....	21
Table 4. All parametric studies applied on the modeled honeycomb structure. ....	30
Table 5. illustration of partarametric study of honeycomb structure. ....	31
Table 6 optimization input for the topology (HCA) method .....	53

## LIST OF FIGURES

Figure 1. a) Buckled beam in two stable pattern b) negative stiffness honeycomb with multiple columns and rows, and c) conventional hexagonal honeycomb [2].....	2
Figure 2. Stress-strain curve for a honeycomb in in-plane compression [3]. .....	3
Figure 3. prefabricated double beam with a central elastic connector.....	7
Figure 4. (a) Shock isolation system with a beam and compression springs in parallel	8
Figure 5. Negative stiffness beam in Klatt’s study [9]. .....	9
Figure 6. Experimental results for a single negative stiffness element [9].....	9
Figure 7. Prefabricated curved beam geometry Qiu's [7]. .....	10
Figure 8. Force-displacement curve for a second mode-constrained curved beam [7]. .....	11
Figure 9. (a) Negative stiffness honeycomb structure [12] and (b) Different metamaterial honeycomb structure under tension [13].....	12
Figure 10. (a) Modeled negative stiffness honeycomb structure, and (b) Geometry of revised negative stiffness unit cell [17]. .....	16
Figure 11. Finite Element model (FEM) of NSH structure.....	17
Figure 12. Modeled unit cell honeycomb (a) 4-unit cell (b) 5-unit cell (c) 7-unit cell. .....	20
Figure 13. Beam thickness (a) thickness of 12.7 mm (b) thickness of 19.05 mm (c) thickness of 6.35 mm. ....	21
Figure 14. Modeled honeycomb in LS-DYNA.....	23
Figure 15. Force-displacement relationship of the modeled and referenced honeycomb structure [20].....	24
Figure 16. Deformed model in LS-DYNA simulation. ....	24
Figure 17. Force-displacement response of three different material. ....	25

Figure 18. Force-displacement response of different beam thickness. ....	27
Figure 19. Force-displacement relationship of applying different unit cell of honeycomb structure. ....	28
Figure 20. Force-displacement relationship of C4-T6.35mm on the honeycomb model. .....	32
Figure 21. Force-displacement relationship of C4-T12.7 mm on the honeycomb model. .....	33
Figure 22. Force-displacement relationship of C4-T19.05 mm on the honeycomb model.....	34
Figure 23. Force-displacement relationship of C5-T6.35 mm on the honeycomb model. .....	35
Figure 24. Force-displacement relationship of C5-T19.05 mm on the honeycomb model.....	36
Figure 25. Force-displacement relationship of C7-T6.35 mm on the honeycomb model. .....	37
Figure 26. Force-displacement relationship of C7-T12.7 mm on the honeycomb model. .....	38
Figure 27. Force-displacement relationship of C7-T19.05 mm on the honeycomb model.....	39
Figure 28. FEA model of the 4-unit cell (a) beam thickness of 6.35 mm (b) beam thickness of 12.7 mm (c) beam thickness of 19.05 mm.....	50
Figure 29. FEA model of the 5-unit cell (a) beam thickness of 6.35 mm (b) beam thickness of 12.7 mm (c) beam thickness of 19.05 mm.....	51
Figure 30. FEA model of the 7-unit cell (a) beam thickness of 6.35 mm (b) beam thickness of 12.7 mm (c) beam thickness of 19.05 mm.....	51

Figure 31 HCA algorithm- LS topology optimization [32] .....	52
Figure 32 Knee bumper application.....	53
Figure 33 Optimized design of the knee bumper.....	54
Figure 34 Convergence diagram, displacement and mass constraints for the optimized topology method (HCA) .....	55

## CHAPTER 1: INTRODUCTION

### 1.1 Background

Impact forces and mechanical vibration are commonly applied daily in most of mechanical systems. Mechanical engineers face a significant difficulty in mitigating these forces to prohibit from harmful products or harming the operators. As a result of its beneficial mix of lightweight stiffness, strength, honeycombs are commonly utilized in packaging, vibration damping, transportation, aerospace (jet engines, rockets, and propellers) and in automotive production. However, the main drawback of honeycomb is its ability to absorb impact energy is highly dependent on the plastic deformation, rendering protective equipment constructed from conventional honeycombs useless for subsequent impacts. Honeycombs with negative stiffness, as presented in this work, are produced to deliver force and energy Normal honeycomb absorption capacity in a recoverable way[1].

When a beam buckles because of a compressive force, this is a simple example of negative stiffness. Figure 1(a) shows that the buckled beam can be configured in two stable ways (first and second stable configuration (solid line) and (dashed line) respectively). Whenever the beam is subjected to a force perpendicular to the beam, a stable configuration can be transformed into another. A beam's force threshold defines how much force it can sustain before snapping into a stable alternative position.

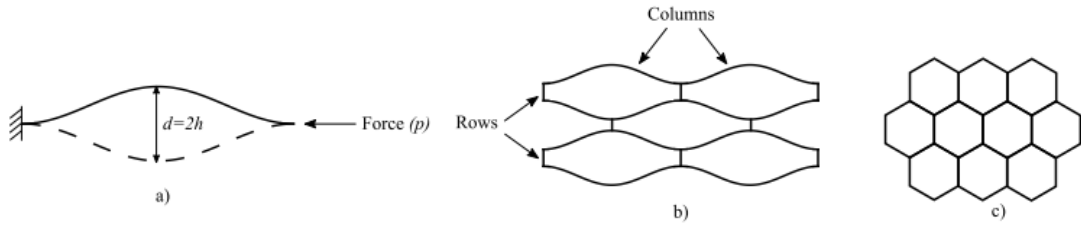


Figure 1. a) Buckled beam in two stable pattern b) negative stiffness honeycomb with multiple columns and rows, and c) conventional hexagonal honeycomb [2].

Honeycomb structures with negative stiffness, as demonstrated in figure 1(b), offer various advantages over conventional materials. In the force-displacement graph, they exhibit relatively long plateaus, making them suitable for force and energy absorption. In addition, their deformation is fully recoverable, which means their force threshold capabilities are not limited to an individual use. Besides, the conventional honeycomb structure has a plateau region as shown in the stress-strain diagram (figure 1(c)). While structures of conventional honeycomb deform in a plastic form, NSHs deform in an elastic mode as illustrated in figure 2. As a result, traditional honeycombs can only be used once for any quasistatic loading. Alternatively, NSHs can be exploited several times. Thus, NSHs are widely applied in repeated loading and unloading applications [2]. This research examines the behavior of these negative-stiffness honeycombs and studies the mechanical performance of applying different scenarios on modeled NSH structure.

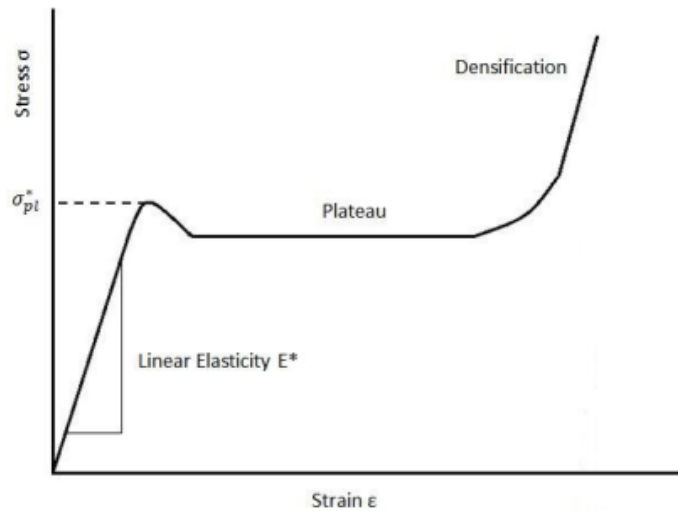


Figure 2. Stress-strain curve for a honeycomb in in-plane compression [3].

### 1.2 Problem statement

Conventional honeycomb structure is type of structure that can sustain the impact of load applied on the structure only once that means it is single use structure. Considering environment and waste of material and cost constrains, single use structure is not recommended option in many applications such as production, packaging, transportation, and damping systems which requires lot of resources to produce normal honeycomb structure. To be able to model structures that are appropriate for multiple use and sustain the force and impact load, Negative stiffness behavior in honeycomb structure is implemented. Negative-stiffness mechanisms are those that can, during some region of their force-displacement relationship, exhibit increasing displacement with decreasing force. accordingly, traditional honeycombs can only be used once for any quasi-static loading while NSHs can be exploited several times.

### 1.3 Research objectives

The thesis study aims to study the mechanical response of different parameters (Material type, unit cell, and beam thickness) applied on the modeled negative stiffness honeycomb structure.

In this thesis, following objectives considered to achieve the aim of the study:

- To develop negative stiffness honeycomb structure that has the same force threshold as previously studied NSHs.
- Validating the modeled honeycomb structure with pervious studied negative stiffness honeycomb model.
- Investigate the force threshold and its effect on different variables applied on the NSH models.
- Determine a relationship between the force threshold to displacement performance of all proposed honeycomb structures.

### 1.4 Thesis layout

The thesis discussion divided into five chapter as follows:

Chapter 1: Describes briefly negative stiffness of honeycomb structure and its concept. Also, first chapter includes problem statement, the aim of the research and objectives and thesis layout.

In the second chapter, literature review will contain all studies and pervious work conducted in the negative stiffness honeycomb (NSH) structure. Both numerical and experimental analysis will be reported in the thesis including pre-curved beam that is used in NSH structure and analytical solution for the curved beams. Also, findings of pervious researchers applied on negative honeycomb structure will be addressed.



Then, chapter 3 present the methodology and approaches used in this study. The finite element modeling is discussed, and LS-Dyna and SolidWorks software will be used to model the honeycomb structure which will be considered according to referenced research. The geometry of the revised negative stiffness model with boundary conditions and control in simulation software on the model will be applied to validate the model. Also, three different variables which are material of NSH, beam thickness and unit cell number on the honeycomb structure are addressed comprehensively. Parametric study explains the methods that will be applied using three subcategories of each variable which will generate multiple models that will be implemented in LS-Dyna simulation to investigate the force threshold behavior.

Accordingly, chapter 4 demonstrate the results and discussions of the modeled honeycomb structure with all simulations applied in LS-Dyna. First, the finite element model validation results will be explored, then the force effect under displacement loading will be examined by changing three studied materials on the honeycomb structure. After that, the effect of applying different beam thickness on the validated honeycomb model will be considered and results will be discovered. Moreover, results of applying 4-, 5- and 7- unit cell number on the honeycomb model will be discussed. Finally, the results of all models in the parametric study will be investigated.

In chapter 5, summary will be provided that will show all main outcomes of the study and conclusion of each result obtained in the study will be discussed briefly. Further studies and recommendations to support the findings of the study.

## CHAPTER 2: LITERATURE REVIEW

### 2.1 Introduction

Negative stiffness was originally noticed in structural engineering because of the phenomena of column instability, which was considered a failure mode since it lost its solidity through a quick rise in strain [4]. Negative stiffness innovation has proven an appealing choice for suppressing vibration at low recurrence excitations, providing linear isolators with load bearing capabilities [3], [5]. Besides, Lakes et al. determined that combinations together with negative firmness incorporations in a visco-elastic lattice could be beneficial into actual circumstances in which the goal is to increase both solidity and damping. They discovered, however, that unstable manner of the innovation behavior occurs if there is no combination of positive stiffness portion [6]. Debeau et.al [2] studied the impact behavior of NSH structures. NSH has been demonstrated to absorb energy during collisions at a constant and low force threshold. This is due to the impact duration being extended in time and the peak acceleration being reduced during the impact. The force threshold is related to the number of negative stiffness cell columns in the NSH structure, whereas the energy absorption capability is proportional to the number of negative stiffness cell rows, as established by FEA and tests with aluminum and nylon NSHs.

### 2.2 Prefabrication curved beams and relationships

According to Qiu's theory [7], third mode buckling could replace second mode buckling if a double beam was rigidly clamped at the center. A prefabricated double beam with an elastic vertical connector at the center is shown in Figure 3. Because of the double beam construction, the beam snaps from one stable position to another while transitioning through a third mode shape, resulting in negative stiffness behavior.

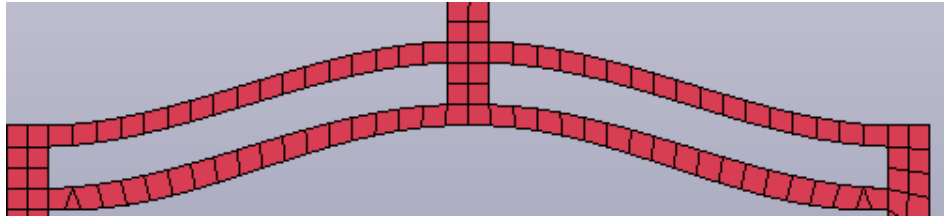


Figure 3. prefabricated double beam with a central elastic connector.

Fulcher [8] investigated the use of a buckling beam with parallel compression springs for shock isolation. A system that allows for variable compression of a beam was used and produced by selective laser sintering (SLS) using nylon 11 in his studies (PA 11). The configuration also allows for up to four compression springs to run parallel with the beam. Figure 4(a) depicts the whole shock isolation system, as well as the projected and observed force-displacement response. The experimental findings as shown in figure 4(b) of the tested beam show negative stiffness behavior in different phases (displacements) in all variations of the tested beam. Furthermore, the graph shows that for an increase in beam compression, more force threshold and more negative stiffness behavior can be noticed from the shock isolation system.

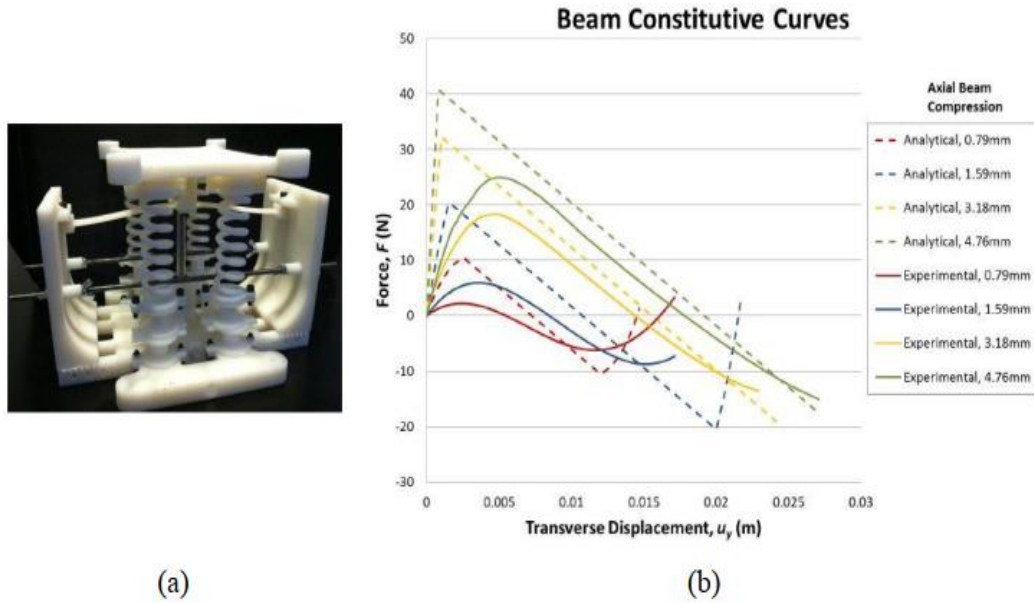


Figure 4. (a) Shock isolation system with a beam and compression springs in parallel and (b) Experimental results from displacement-controlled loading [8].

The use of negative stiffness beams in near-ideal shock absorption has been demonstrated in previous research. While these negative stiffness elements have been designed either as standalone structures or as components of shock isolation systems, they have not been widely assembled in a periodic honeycomb-like arrangement. This research explores this possibility.

Beams with negative stiffness allow energy dissipation when deforming from one shape with first modal buckling to another while exhibiting negative stiffness behavior. They tend to have high-level initial stiffness and provide near-ideal impact isolation at the designed force threshold. A performance evaluation of a single beam with negative stiffness was published by Klatt et al.[9], According to Fulcher et al., Kashdan et al. and Qiu et al. studies [7], [10], [11], Kratt et al. showed that a prefabricated curved beam as in figure 5 can be applied as a negative stiffness behavior like that typically exhibited by a straight beam that buckles from an axial load.

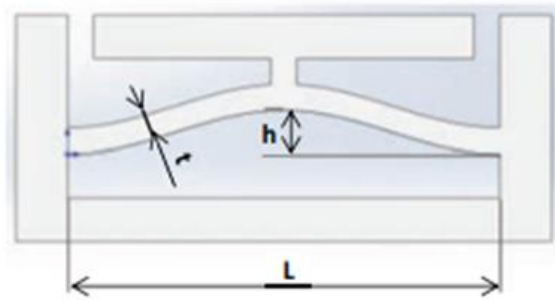


Figure 5. Negative stiffness beam in Klatt's study [9].

In addition, Klatt performed compression tests on the pre-curved beams fabricated by selective laser sintering. Figure 6 shows the obtained results experimentally in the Klatt study [9]. A beam that undergoes a loading path that exhibits exceptionally low stiffness is shown in Figure 6. Additionally, the beam deforms in a different direction during unloading and loading, suggesting that energy dissipates within it.

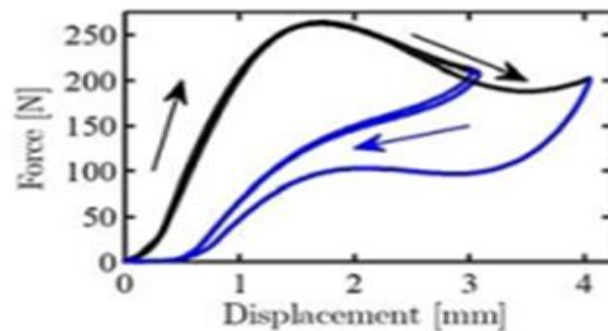


Figure 6. Experimental results for a single negative stiffness element [9].

Qiu's [7] design and Klatt's [9] experimental evaluation of nylon 11 was adopted as a model for the prefabricated buckled beam. Figure 7 illustrates the beam design. The equation 3.1 describes the shape of a beam of length  $l$ , thickness  $t$ , width  $b$ , and initial height at apex  $h$ .

$$\bar{w}(x) = \frac{h}{2} \left[ 1 - \cos\left(2\pi \frac{x}{l}\right) \right] \quad (\text{eq.1})$$

The equation (eq.1) gives a lateral position (x) for any point on a beam from one end and a vertical distance  $\bar{w}(x)$  from the horizontal line connecting the two ends.

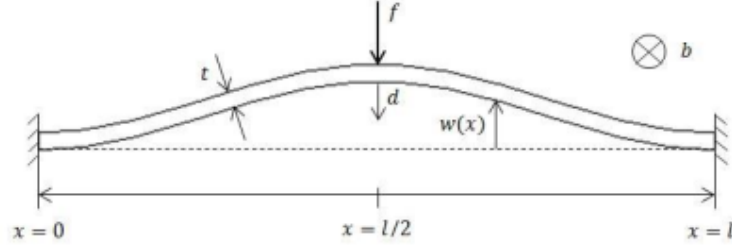


Figure 7. Prefabricated curved beam geometry Qiu's [7].

For a prefabricated curved beam, Qiu [7] also developed analytical relationships between transverse force and displacement. From the relationships derived, following equations obtained for a beam in as second mode of bending is restricted:

$$F_1 = \frac{3\pi^4 Q^2}{2} \Delta \left( \Delta - \frac{3}{2} + \sqrt{\frac{1}{4} - \frac{4}{3Q^2}} \right) \left( \left( \Delta - \frac{3}{2} - \sqrt{\frac{1}{4} - \frac{4}{3Q^2}} \right) \right) \quad (\text{eq.2})$$

$$F_3 = 8\pi^4 - 6\pi^4 \Delta \quad (\text{eq.3})$$

$$\Delta = d/h \quad (\text{eq.4})$$

where Delta ( $\Delta$ ) represents transverse displacement, d, normalized by the apex height, h, and Q represents the ratio between h, the apex height of the beam, and t, the beam in-plane thickness. Furthermore, from the normalized force, the actual force F that acts on the beam can be defined by using the equation

$$f = \frac{FEIh}{l^3} \quad (\text{eq.5})$$

where  $E$  represents the material Young's modulus and  $I$  represent the cross-sectional moment of inertia and  $L$  represent the length of the beam. Figure 8 demonstrates a description of a conventional force-displacement scenario of a negative stiffness beam with a second mode constrained.

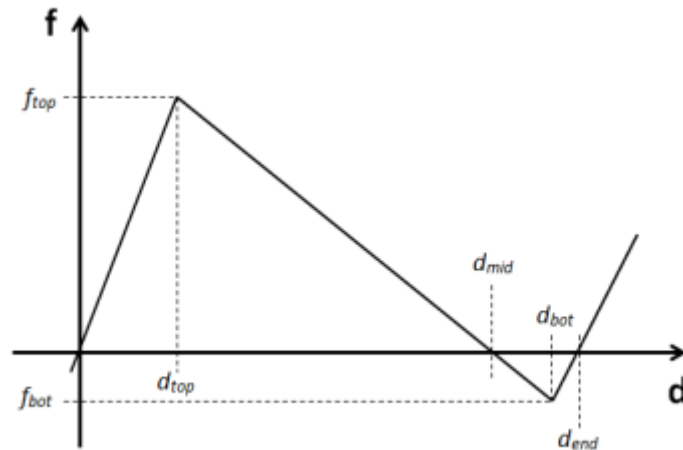


Figure 8. Force-displacement curve for a second mode-constrained curved beam [7].

### 2.3 Negative stiffness honeycomb structures

As shown in Figure 9(a), Correa et al. [12] have developed honeycomb structures with negative stiffness composed of prefabricated buckled beams arranged in multiple rows and columns. Selective laser sintering was used for manufacturing the two honeycomb prototypes. NSH structures recovered their initial profiles with minimal plastic deformation when compared with regular honeycomb structures. An estimated 65% of the energy input was dissipated through the system. The NSH structure is formed by snapping units arranged in a regular pattern, which Rafsanjani [13] investigated under tension loading. Figure 9 (b) illustrates how NSH structures behave under tension loading. Based on the results, different nonlinear mechanical responses could be generated by tuned NSH structures.



Figure 9. (a) Negative stiffness honeycomb structure [12] and (b) Different metamaterial honeycomb structure under tension [13].

Tan et al. [14] examined the structure of a cylinder honeycomb occupied by projecting beams. The results revealed that cylindrical arrays can dissipate energy under displacement loads, but the force thresholds were same as honeycombs with negative stiffness. The composite system comprised of pre-buckled beams with polymer material matrix was experimentally examined by Cortes et al. [15] during uniaxial compression, the strength of the material is measured, as well as its energy dissipation. To increase stiffness and energy absorption of the system due to negative stiffness (pre-buckled beams), matrix construction is used. Highest strain experienced by the beam before buckling was referenced for a design. Using a negative stiffness matrix, we found that stiffness and energy dissipation were improved by ensuring that the beam stiffness was precisely matched to the matrix stiffness before buckling.

The multiple tetra beam lattice presented by Ha et al. [16] was found to absorb energy when moving from one position to another via negative stiffness behavior. To create the lattice, a 3D selective laser sintering method was employed. Large deflections in the multiple tetra beams created geometric nonlinearity and, as a result, negative stiffness behavior. The inclined angle and the beam slenderness ratio served as the



foundation for the tetra beams unit's design criteria. The design criteria were used to tailor the lattice unit's energy dissipation capacity and force threshold performance. However, the system's energy dissipation and force thresholds were comparable to those of pre-buckled structures.

Under quasi-static loads, Debeau et al. [2] studied the mechanical performance of negative stiffness honeycombs. In the study, Correa et al. [17] used selective laser sintering (3D printing) to create the honeycomb using the negative stiffness concept. The study included modeled negative stiffness honeycombs made from aluminum as well, to evaluate the behavior of other materials. Several drop mass tests were conducted on both honeycombs with negative stiffness, and the findings indicated that the honeycombs may be utilized for shock isolation provided that mechanical energy delivered to the honeycomb does not exceed its ability to dissipate energy. Also, Debeau et al. [2] reported that, although most studies have focused on the quasi-static evaluation of honeycomb structures, an experimental investigation was carried out into the mechanical behavior of negative stiffness honeycombs when subjected to impact and quasi-static loading. Like what Correa et al. [17] investigated, the negative stiffness honeycomb was made from nylon by 3D printing selective laser sintering. However, an additional negative stiffness aluminum honeycomb was used in the study to examine the behavior of various materials.

A metamaterial structure with negative Poisson's ratio and stiffness behavior has been proposed by Hewage et al. [18] in a study that linked two unnatural properties. An experimental evaluation and analytical modeling of the proposed system were conducted using a negative Poisson's ratio assembly that stabilized negative stiffness elements. To demonstrate how three changes for metamaterial elements with negative

stiffness design show how composite structures based on its stiffness and Poisson's ratio exhibit direction reversal simultaneously in both axial and lateral dimensions, evaluated in the specified range of strain under displacement loading on the host assembly value. Such composite systems have demonstrated capacity to improve properties like vibration damping for transportation, defense, operational applications, and applications in the space field.

Recent studies [19]–[31] show that structures with negative stiffness can provide extreme vibration and sound absorption capabilities. These structures with negative stiffness are therefore strong candidates for constructing novel metamaterials for noise suppression, anechoic coatings, and substrates of broadband imagers. Results of dynamic experiments showed that a simple negative stiffness system could increase the damping of the system and tune the dynamic behavior. Quasi-static measurements showed that the permeability of the curved beam is finite and positive at low frequencies. This indicates that the system works on a wide frequency spectrum than most negatively stiff mechanical meta-material inclusions.

In this study, a model was developed using finite elements analysis software (LS-Dyna). By applying the validated model, the maximum force in a system can be predicted by the instability of elements with negative stiffness as it transitions from one stable mode to another.

## CHAPTER 3: METHODOLOGY

### 3.1 Introduction

Negative stiffness structures and their design have been the subject of substantial research, as discussed in the preceding chapter. As part of this chapter, negative stiffness beams are arranged in various combinations to explore their effects using FEA. This is accomplished by analyzing negative stiffness model formed and studied by correa et.al [12] in FEA under quasi-static displacement loading and validating it with the modeled honeycomb structure in this study. Accordingly, the verified model is used further in the study to examine the mechanical performance of the negative honeycomb structure behavior in various models. Then the effects of applying different variables (material, beam thickness, and unit cell) in a honeycomb structure are evaluated. the conclusion will provide a basis for modeling future honeycombs based on the results of these investigations. So that, these honeycomb structures can be applied in applications include road bumpers and protective devices (helmets and bicycle seat) and packaging during transportation.

### 3.2 Finite Element Modeling

A model was imported from SolidWorks software and used in finite element modeling software (LS-Dyna). In LS DYNA, the finite model of the negative stiffness honeycomb (NSH) structure tested by correa is validated by applying exact dimensions and properties analyzed in Correa et al. model [12]. Various models were developed as discussed in detail in section 3.3 after the FEM was validated, to investigate the effect of different NSH parameters, including the structure thickness, multiple honeycomb units as well as different material types of negative- honeycomb structures.

### 3.2.1 Model geometry

Honeycomb structure for negative stiffness, as shown in Figure 10(a), with 5-unit cell of double buckled beams, was formed with SolidWorks, and then imported to LS-DYNA. To prevent second mode beam buckling, a vertical line links in between each double buckled beam when it shifts from one position to another according to Correa study, thereby ensuring beam instability. Based on the model done by correa et. al [12], the unit cell dimension is illustrated in Figure 10(b). The total unit cell length with two side walls is 55.88 mm and internal unit cell length is 50.8 mm, the vertical height of each unit cell is 20.32 mm with thickness of each beam is 1.27 mm and two beam are set to be double beam with vertical line in the middle for thickness of 1.27 mm. the geometry of negative stiffness unit cell shape is combination of rectangular and oval constructed in different arrangement to generate negative stiffness behavior of desired honeycomb structure.

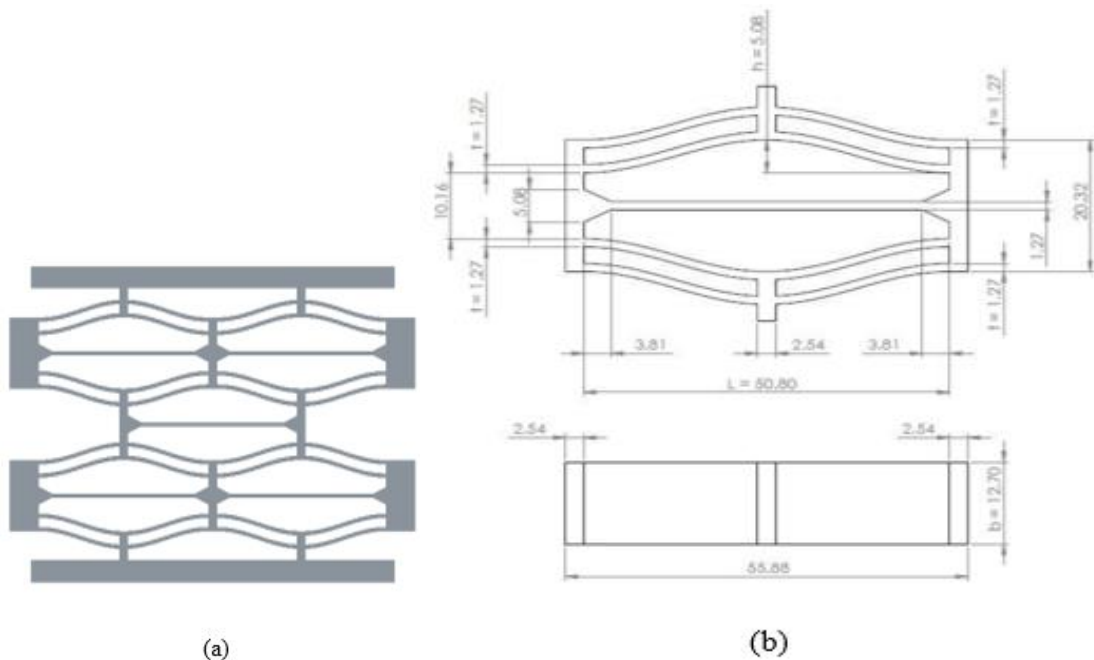


Figure 10. (a) Modeled negative stiffness honeycomb structure, and (b) Geometry of revised negative stiffness unit cell [17].

In Figure 11, the model in LS-Dyna represents the negative stiffness honeycomb structure was formed with the same dimension of referenced paper and was used in validation. The quasi-static analysis (displacement load analysis) was simulated by applying two steel plates as support for the shaped model, one plate was constrained as fixed support, while the second plater was used as displacement load receiver (Impactor). The lower part was constrained from x, y, z -displacement direction and in x, y, z rotational direction, while for the impactor movement was allowed in y-direction and constrained from all other direction x and z direction. Also, the negative honeycomb model was also constrained from x, z rotational and translation direction and movement on the y-direction only as its was quasi-static loading.

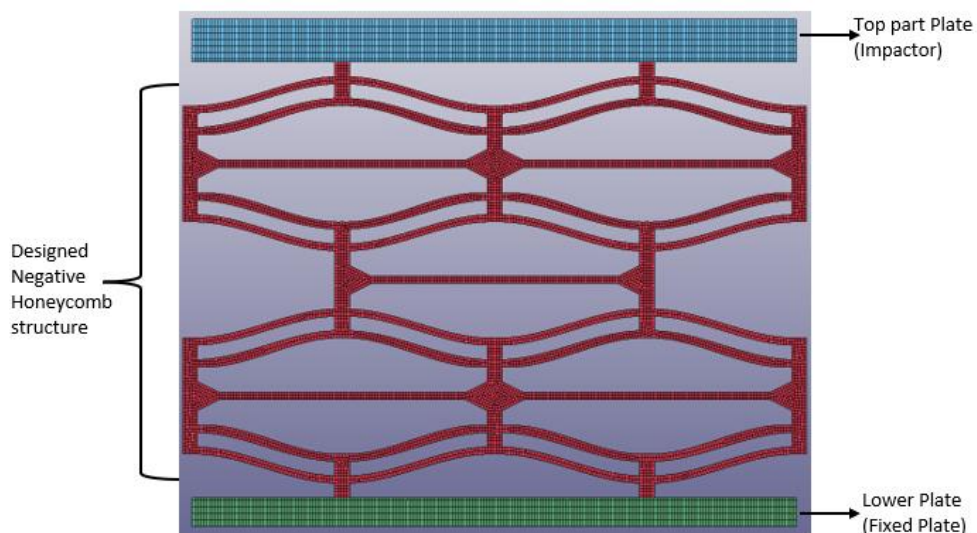


Figure 11. Finite Element model (FEM) of NSH structure.

### 3.2.2 modeling of material

The applied material for the modeled NSH in LS-DYNA is Nylon 11. The Nylon 11 is widely used in normal honeycomb structure and recently been used for negative stiffness honeycomb structure as it has higher strength, better heat resistance, lower impact on environment and during production it utilizes fewer renewable resources.

Steel plates were modeled as upper loading plates and lower base plates. As shown in Table 1, input values of yield stress, Poisson's ratio, density, and young's modulus were applied for the Nylon11 and steel material model.

Table 1. Material properties of applied materials on the model.

Property	Steel	Nylon 11 (PA 11)
Density (D) $kg/m^3$	7830	1040
Poisson's Ratio (PR)	0.30	0.33
Young's Modulus (E) MPa	2e+05	1582
Yield Strength (SIGY) MPa	320	250

Material properties of selected material are listed in Table 2. Based on referenced paper [12] simulation nylon 11 was used, and nylon 6/6 with nylon 12 were applied as other two materials since there are widely used after nylon 11 to investigate the effect of applying change in material on the model.

Table 2. properties of the selected materials in this study.

Property	Nylon 6/6	Nylon 11	Nylon 12	Steel
Density (D) $kg/m^3$	1140	1040	930	7830
Poisson's Ratio (PR)	0.33	0.33	0.33	0.30
Young's Modulus (E) MPa	1900	1582	1650	2e+05
Yield Strength (SIGY) MPa	250	250	250	320

### 3.2.3 Boundary conditions and control

Since neither type of element (beam element and shell element) applied showed significant differences in results from trials investigations, the beam element was selected to reduce the run time for the finite element model and to avoid hourglass energy effects when using an under-integrated shell element. To compress the

honeycomb structure, nodes of the lower base plate were assigned displacements of 25 mm in y-direction. The lower plate was constrained in all directions unlike the impactor where nodes were only constrained in both z and x directions, and roller constraints were applied in the corners of the modelled negative stiffness honeycomb structure.

#### *3.2.4 Validation of the honeycomb model*

To validate the referenced model, a model in Figure 11 was developed according to the dimension of referenced model as sketched in Figure 10. The beam thickness of 12.70 mm and full model height of 76 mm was shaped. Then, applying boundary condition and lower plate was fixed (constrained), honeycomb structure was assigned as constraint and only movement in the negative y-direction was selected. A roller constraint applied on the side honeycomb model to allow it to rotate in the y-direction only as the study is using quasi-static (displacement) analysis in one direction only. Finally, the displacement load was distributed equally on the upper part (impactor) of the model with a displacement loading of 25 mm and the model simulation was ran through LS-Dyna run.

### 3.3 Parametric study for the negative stiffness honeycomb model

After validating the model, the effect of applying change in three different parameters of modeled negative stiffness honeycomb are studied. The three parameters (material type, unit cell of honeycomb structure and beam thickness) are used in this study, in which each of these parameters has three variables which lead to almost 27 simulations to be addressed in the thesis. Each variable corresponding to each parameter is considered in LS-DYNA simulation as per formed honeycomb structure and then the variables is used as inputs in the simulation to study the negative stiffness performance of the model. The three-material applied are nylon 6/6, nylon 11 and nylon 12 and each

material has its mechanical properties as presented in table 2. Figure 12 shows the three different unit cell applied in the FEA model (4-,5- and 7-unit cell respectively). Three beam thickness of 6.35mm, 12.7 mm and 19.05 mm were applied in the model and Figure 13 pointed the beam thickness location in the modeled honeycomb structure.

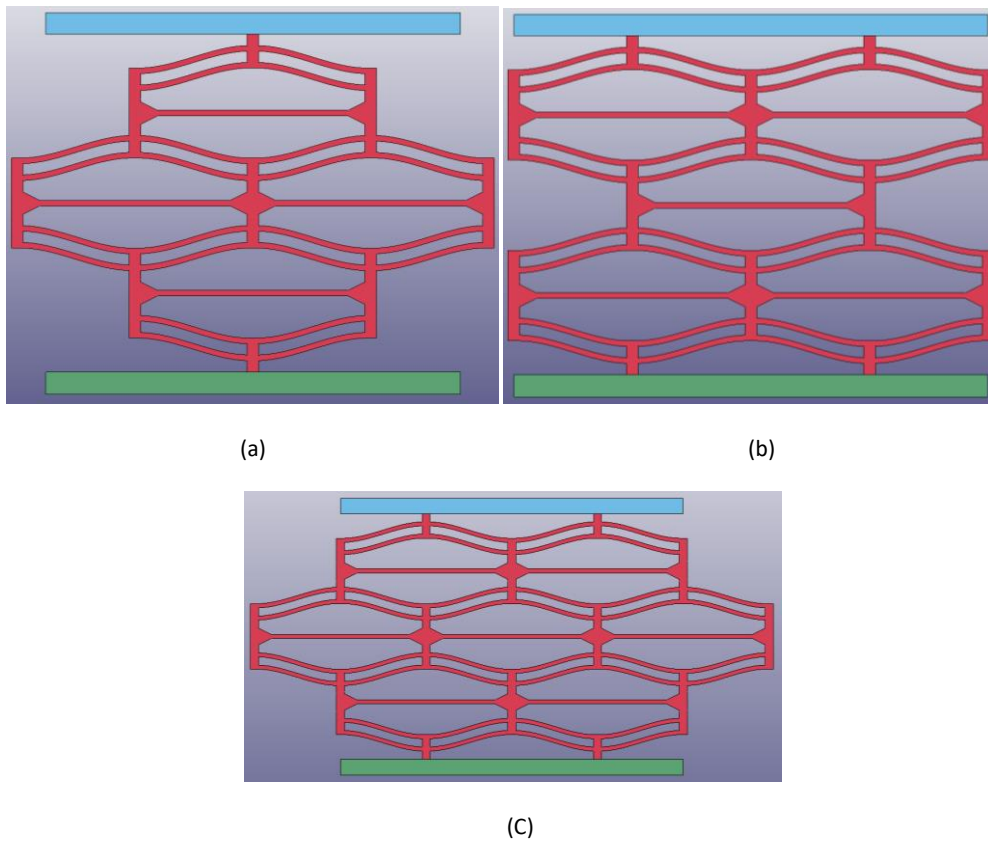


Figure 12. Modeled unit cell honeycomb (a) 4-unit cell (b) 5-unit cell (c) 7-unit cell.

It is important to note that the beam thickness significantly influences the negative stiffness of buckled beam structure. The findings of Qiu, beam thickness has a significant effect on stability, which influences negative stiffness behavior. Consequently, three different models of the negative stiffness honeycomb structure were generated to study the effect of changing the beam thickness. In Figure 13, the beam thickness of 6.35 mm, 12.7 mm and 19.05 mm and was modeled in LS-DYNA.



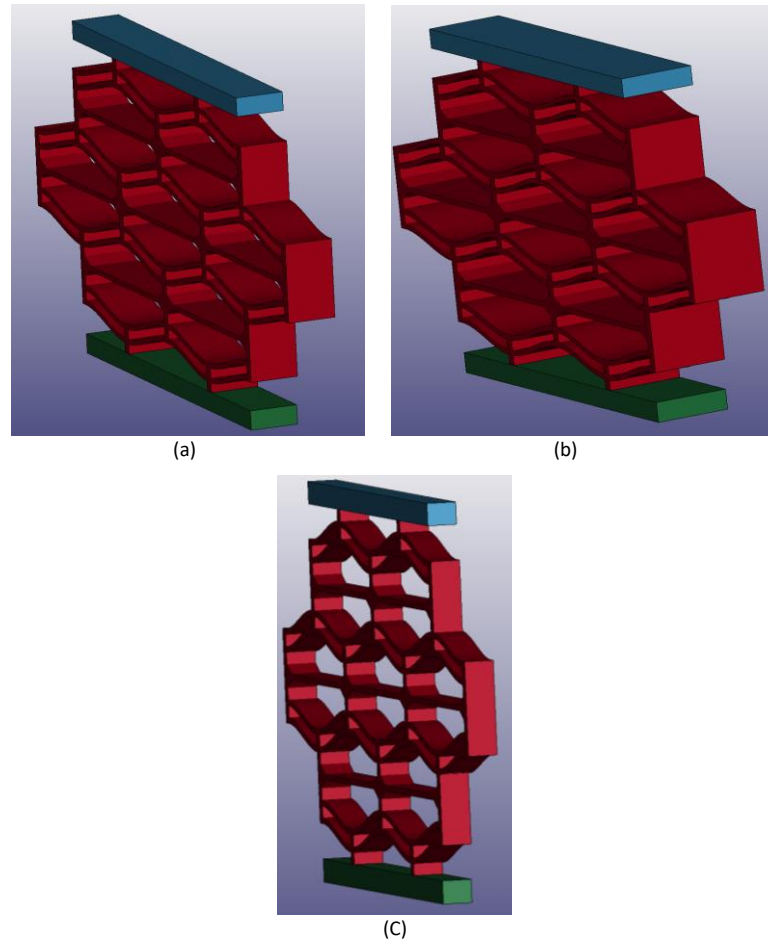


Figure 13. Beam thickness (a) thickness of 12.7 mm (b) thickness of 19.05 mm (c) thickness of 6.35 mm.

Table 3 present the three main variables with three different options for each parameter which are considered in this study to investigate the effect of varying tabled parameters on the modeled honeycomb structure.

Table 3. Parametric study applied on the honeycomb model.

Parameters Options	Material	Unit cell element size (Nos.)	Beam Thickness (mm)
Option 1	Nylon 6-6	4	6.35
Option 2	Nylon 11	5	12.7
Option 3	Nylon 12	7	19.05

## CHAPTER 4: RESULTS & DISCUSSIONS

### 4.1 Model Validation

Finite element modeling (FEM) as illustrated in Figure 14 was validated with reference to negative stiffness honeycomb prototype tested by Correa et al. [12]. Using LS-DYNA, the modeled negative honeycomb was simulated for validation. To idealize the analysis, roller supports for each of the vertical side cell walls was applied on the model, the bottom part (lower plate) was used as fixed support and the upper plate (impactor) was used as displacement loading on it in the y-direction. Figure 15 shows the force vs displacement curve of referenced negative stiffness model which was used to validate the model of negative stiffness honeycomb structure. A quasi-static displacement load of 25 mm was applied on the impactor of honeycomb as the main purpose of this study to investigate the first peak force threshold of the honeycomb structure. In addition, the double beam connectors were assigned as roller support as well to simulate the third bulking mode to achieve the negative stiffness honeycomb perspective in FEM. The material properties were applied according to the referenced values in the referenced model as shown in Table 1. For the honeycomb structure model as referenced model to be nylon 11, bottom fixed plate and top plate (impactor) to be steel. Each negative stiffness region is caused by a row of curved beams transitioning from one first mode buckled to another, then, the layers buckle consecutively. The predicted force-displacement curve from FEA reveals continuous negative stiffness regions as illustrated in **Error! Reference source not found.** As observed from **Error! Reference source not found.**, the force threshold is approximately 289 N before buckling occur while the force is 275 N as per referenced paper which shows strong correlation between the two models with an error of almost 5%. The slight difference in values obtained between two model might be due to material properties of the Nylon

11 as the values which was considered in the validation as listed in Table 1 as per referenced paper are young modulus's, mass density and yield stress, while properties such as Strain rate parameter and tangent modulus were ignored in the study. These values would change the results obtained to match with the desired value of the force threshold.

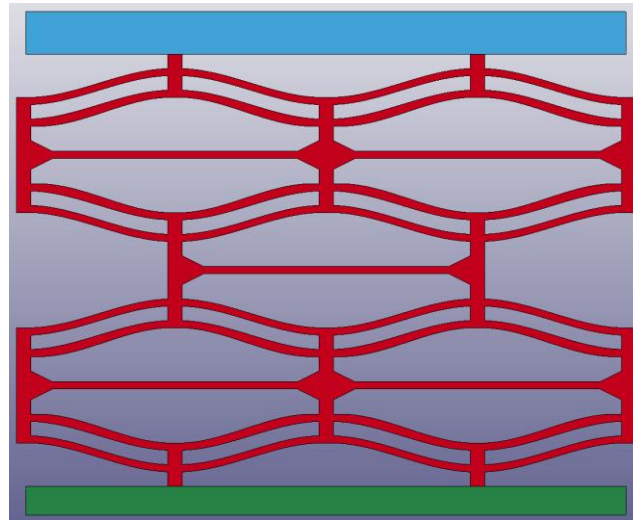


Figure 14. Modeled honeycomb in LS-DYNA.

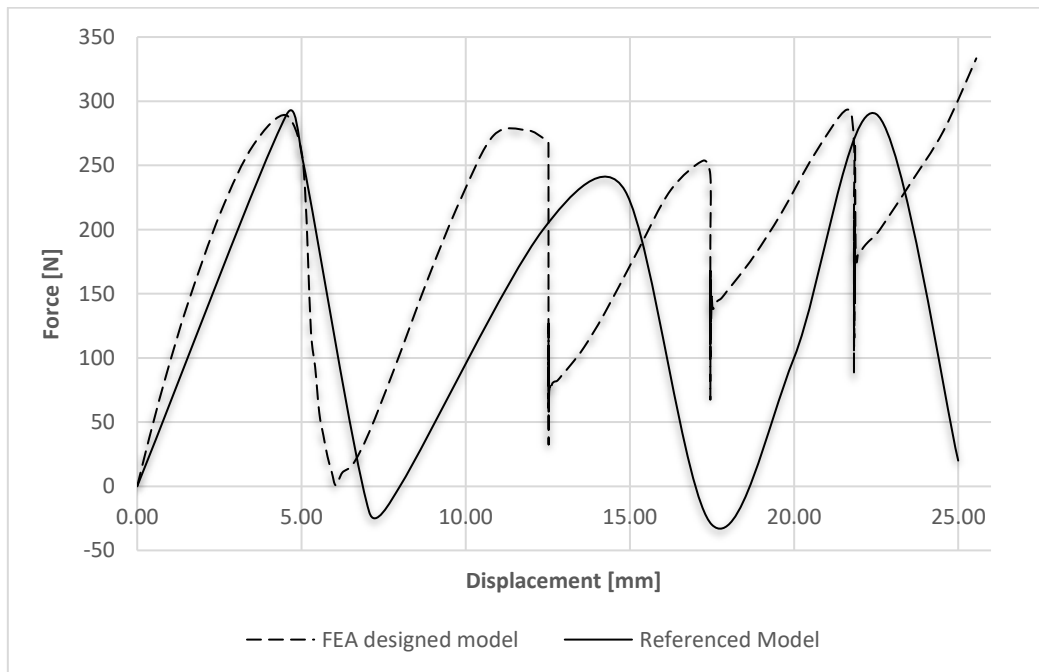


Figure 15. Force-displacement relationship of the modeled and referenced honeycomb structure [20].

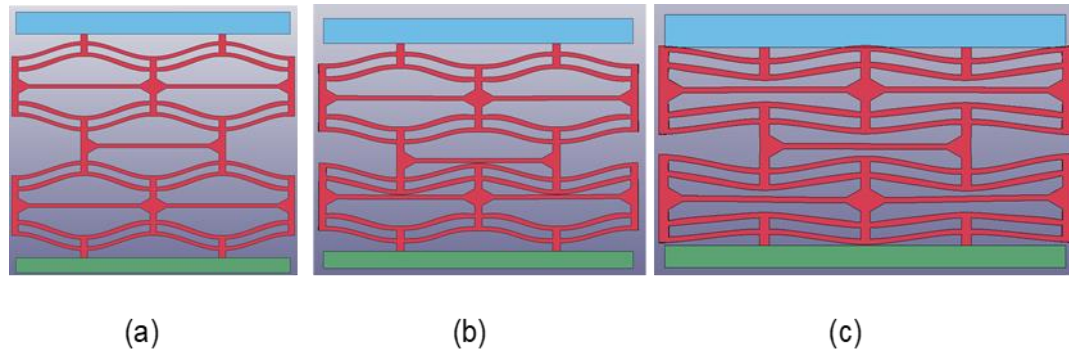


Figure 16. Deformed model in LS-DYNA simulation.

As a result of the validation of the model, the main characteristics of negative stiffness honeycombs were captured. Hence, various structures of the negative honeycomb will be investigated using different parameters which include material type applied in the model, the beam thickness of the negative stiffness model and unit cell number of the model that matching with the referenced geometry as presented in Figure 12 and 13.

#### 4.2 Effect of Material Type

To examine the effect of material type on the negative stiffness honeycomb, the validated model in Figure 15 was used. Three commonly used materials for honeycomb structures are Nylon 11, Nylon 6/6, and Nylon 12 which were used in this study. From LS-DYNA, three different model with the desired materials were created and material properties corresponding to each material (Nylon 6/6 ,11 and 12) were applied in accordance with values reported in Table 2. The loading was idealized by applying fixed support for the bottom plate, displacement loads on the top plate and roller

supports on the side corners were assigned to simulate the model in negative stiffness mode. Young modulus of 1582 MPa and Poisson's ratio of 0.33 were assigned in the three different FEA models. The displacement loading of 10 mm were applied for this simulation as the aim of investigation in this section is to study the force threshold behavior by changing material in the model of negative stiffness honeycomb.

Figure 17 shows force versus displacement curve of nylon 6/6,11 and 12 materials. The referenced material used in validation was nylon 11 as stated in Correa study [12], which was applied in the simulation to address the effect of various type of material on the negative honeycomb structure. The force threshold was approximately 400 N in nylon 6/6, which is higher than nylon 11 and 12 values (around 320 N) at the first peak. However, in the second peak the values of both nylon 6/6 and nylon 12 (650 N and 730 N respectively) were higher than nylon 11 (200 N).

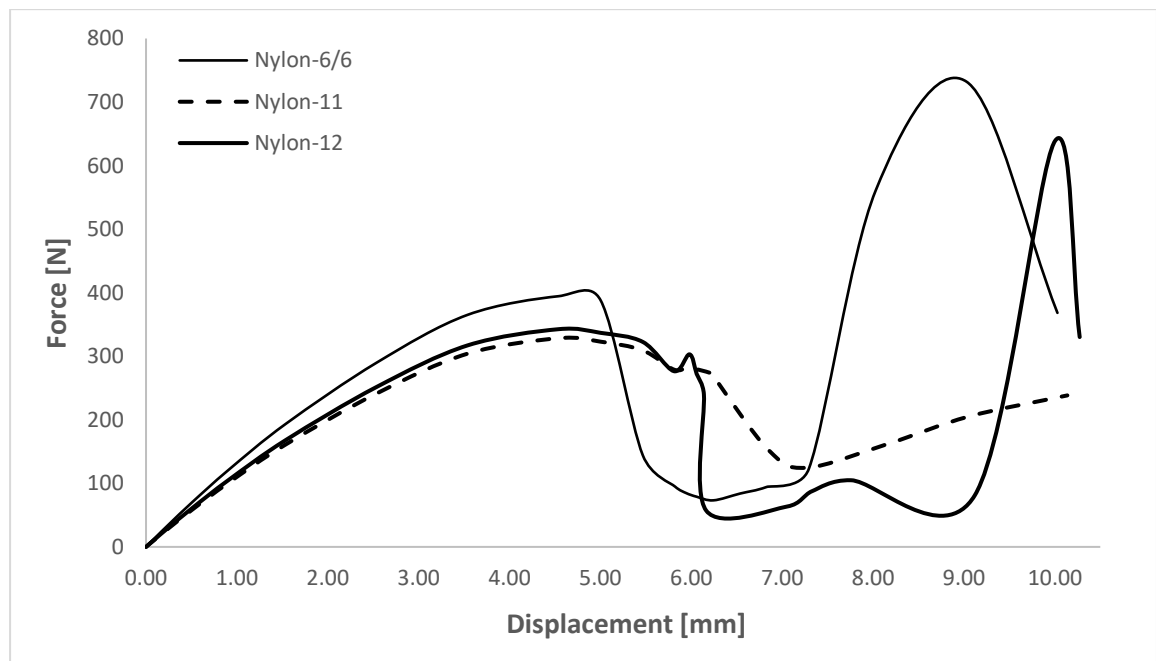


Figure 17. Force-displacement response of three different material.

#### 4.3 Effect of Beam width

The force threshold of almost 500 N represent the buckled beam rows force in beam thickness of 19.05 mm as shown in Figure 18 while, the force value was almost 300 N for beam thickness which is almost half of the force threshold (150 N) of beam thickness of 6.35 mm in the first loading phase. During first unloading phase, the 6.35 mm and 19.05 mm beam thickness shows same force threshold of almost 6 N, however at the beam thickness of 12.7 mm the force was 90 N. In the second peak of the simulation the thickness of 19.05 mm was increasing dramatically and reaches to be same as first peak while, 290 N force was noticed in 6.35mm thickness and 250 N for 12.7 mm beam thickness.

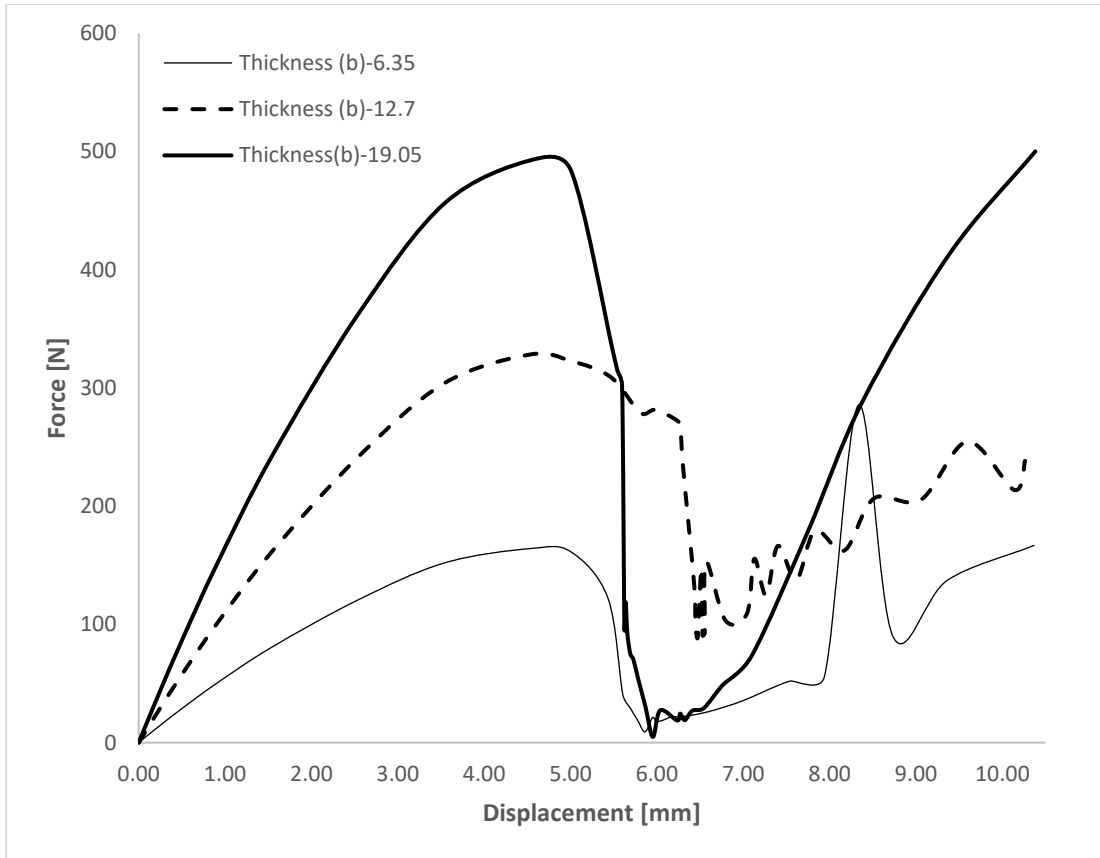


Figure 18. Force-displacement response of different beam thickness.

#### 4.4 Effect of multiple honeycomb unit-cell structure

In the honeycomb structure mentioned previously, the threshold force was approximately 200N. The force threshold may, however, need to be higher in some applications. Changes are available in the geometry of the buckled beams, the configuration of the beams, and the material of the honeycomb are several approaches for increasing the force threshold. To achieve higher force thresholds, it may also be feasible to use multiple honeycomb structures or a honeycomb structure with multiple buckled beams. A finite element model of the modeled honeycomb was developed by applying a different arrangement of unit cells with the same dimensions according to the referenced paper model used in validation to examine the force threshold behavior of using multiple unit cell of honeycomb models. The unit cell of honeycomb is placed

juxtaposed in arrangements to achieve the 4-, 5- and 7-unit cell model respectively. All cells were simulated under displacement loading of 10 mm to study the effect of applying various arrangement and unit cell of honeycomb structure.

Figure 19 shows the force-displacement relationship of the multiple unit cell honeycomb model and reference model [12]. During the loading phase of the honeycomb, the force threshold was the same in the 7-unit cells and 5-unit cells arrangement of honeycomb and was almost half (150 N) for the 4-unit cell model. However, the model showed a higher threshold at which beams started rebounding during unloading in 5- and 7-unit cell model than the 4-unit cell model. As a result, multiple honeycomb units with fixed dimensions, a magnification of the force threshold will occur, depending on their properties.

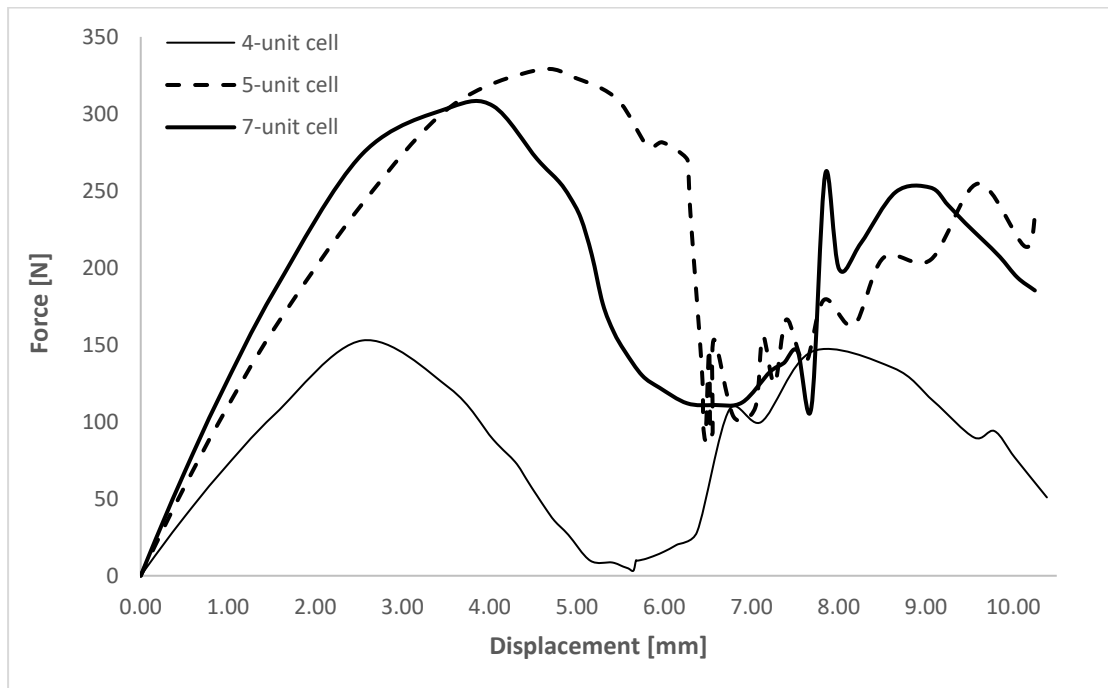


Figure 19. Force-displacement relationship of applying different unit cell of honeycomb structure.



#### 4.5 Results of parametric study

After the referenced model in correa study was validated and investigation were conducted to study the effect of changing material, beam thickness and unit cell respectively of the honeycomb structure, parametric study of the changed variables is applied. In pervious sections, the effect was studied for each variable separately without considering the effect of changing in of other variable. The study in this section includes changing in one variable while fix the other two variables simultaneously and address the force threshold effect on the related simulation. For example, if the unit cell is set to 4-unit cell and beam thickness to 6.35 mm then the material change (nylon 11, etc.) is considered in LS-DYNA simulation and its effect to be studied on the honeycomb model. Table 4 presented the parametric study which is applied in this section of the study.

Table 4. All parametric studies applied on the modeled honeycomb structure.

<b>Unit Cell</b>	<b>Thickness</b>	<b>Material</b>
4-unit cell	T1: 6.35	Nylon-6/6 Nylon-11 Nylon-12
	T2: 12.7	Nylon-6/6 Nylon-11 Nylon-12
	T3: 19.05	Nylon-6/6 Nylon-11 Nylon-12
5-unit cell	T1: 6.35	Nylon-6/6 Nylon-11 Nylon-12
	T2: 12.7	Nylon-6/6 Nylon-11 Nylon-12
	T3: 19.05	Nylon-6/6 Nylon-11 Nylon-12
7-unit cell	T1: 6.35	Nylon-6/6 Nylon-11 Nylon-12
	T2: 12.7	Nylon-6/6 Nylon-11 Nylon-12
	T3: 19.05	Nylon-6/6 Nylon-11 Nylon-12

From Table 4, 27 different simulation was conducted, and three different materials (nylon-6/6, nylon-11, and nylon-12) were chosen to be presented as variables in all runs in LS-DYNA. Thus, figures of force versus displacement relationship are discussed in the following section in this chapter. First, the 4-unit cell model were addressed with three different thickness (6.35 mm, 12.70 mm, and 19.05 mm) and by varying the three materials in each run, the force-displacement response was discussed. Then, same methodology was used for the 5-unit cell model and 7-unit cell model. All models of negative stiffness honeycomb in LS-DYNA used in the thesis study are attached in the Appendix section.

#### *4.5.1 Result for 4-unit cell of beam thickness 6.35 mm*

The unit cell of 4-unit cell of honeycomb was fixed as first parameter and second was thickness of 6.35 mm and three different simulation was applied in three different material type as shown in Table 5 and force with respect to displacement loading of 15 mm was investigated.

Table 5. illustration of partarametric study of honeycomb structure.

Unit cell	Beam Thickness	Material
4-unit cell	T1: 6.35	Nylon 6-6
		Nylon 11
		Nylon 12

Figure 20 shows the results obtained for this section of the parametric study (C4T6.35) which represent the unit cell of four number and thickness of 6.35 mm and Nylon- 6/6 indicates the material type used in this simulation. During the loading, the force

threshold was almost similar (in range of 90-100 N) in the three material used (Nylon6/6, nylon 11 and nylon 12) while in the second peak the nylon-6/6 differs and increased dramatically to reach to 620 N and the force threshold in nylon-12 was about 340 N which almost half compared to nylon-6/6 and also nylon-11 (105 N) and negative stiffness behavior was presented as shown in Figure 20 and the force threshold differs when reaches to 15 mm displacement, it was almost doubled in the nylon-6/6 material compared to nylon 11 and nylon-12.

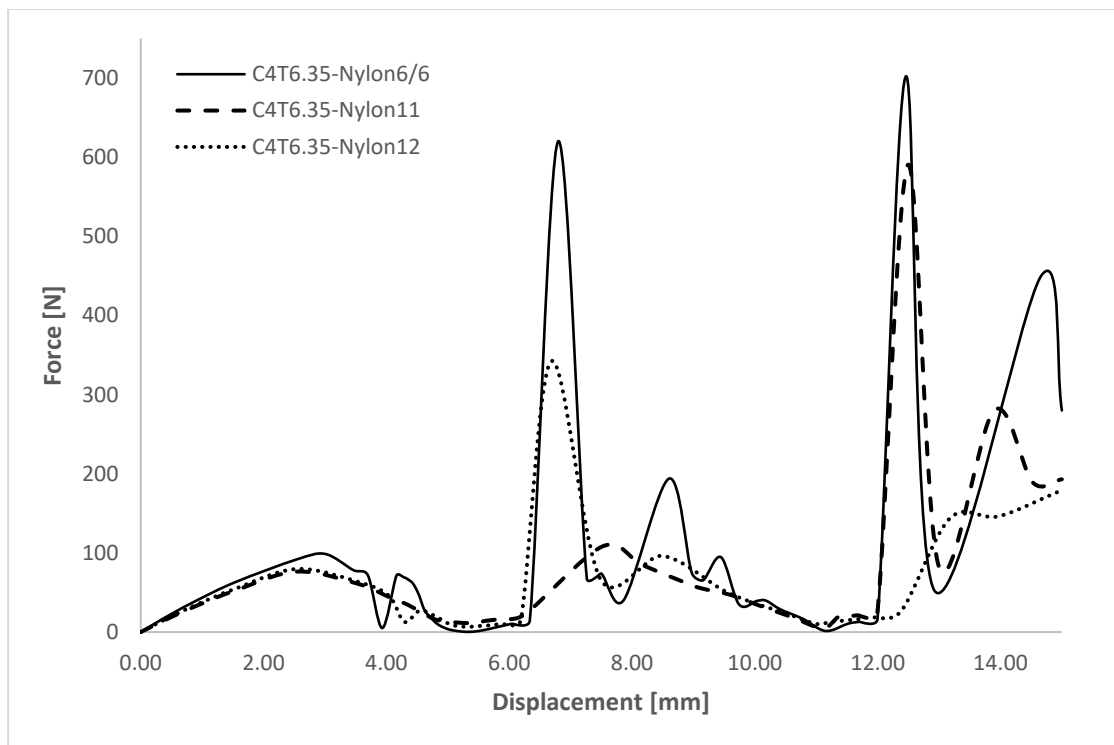


Figure 20. Force-displacement relationship of C4-T6.35mm on the honeycomb model.

#### 4.5.2 Result for 4-unit cell of beam thickness 12.7 mm

The unit cell of 4-unit cell of honeycomb was applied as first parameter and second was thickness of 12.7 mm and three different simulation was utilized for the three different materials (nylon 6/6, nylon11 and nylon12) and force with respect to displacement loading of 15 mm was investigated.

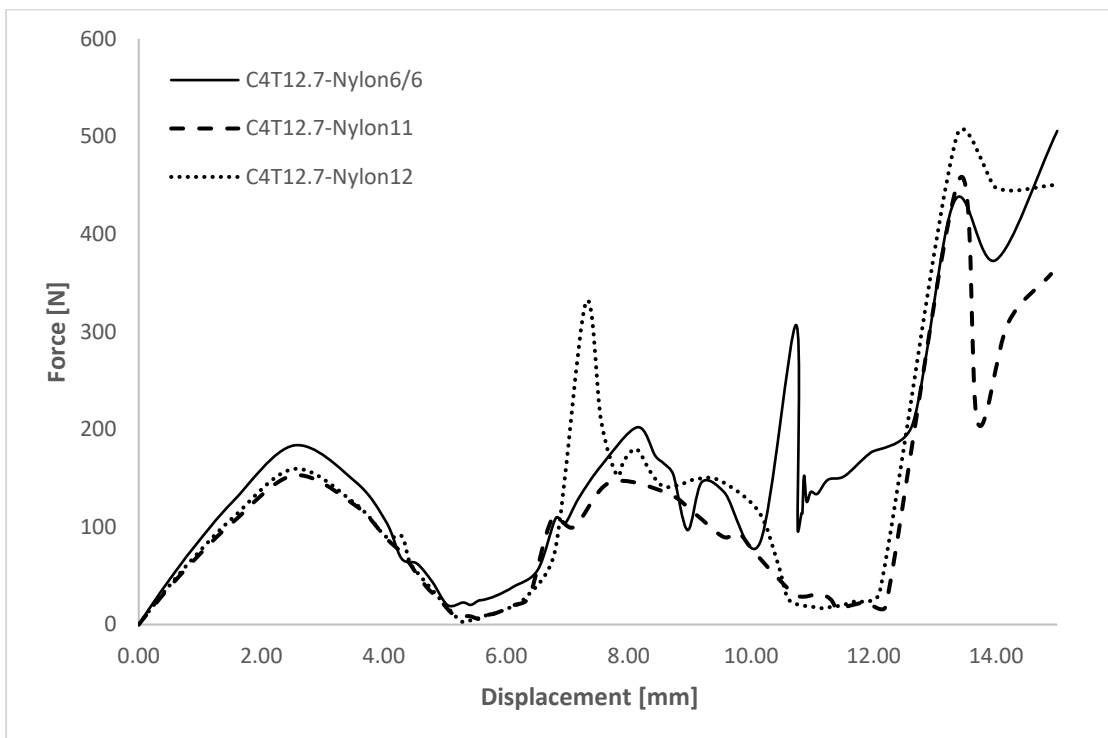


Figure 21. Force-displacement relationship of C4-T12.7 mm on the honeycomb model.

C4T12.7 means the parametric study of 4- unit cell and beam thickness of 12.7 mm as in Figure 21. the force threshold of nylon 6/6 was the highest force (183 N) with an error 15 % compared to nylon 11 and nylon 12 values (153, 159 N respectively). Then, for the second peak, nylon 12 material differs from other nylons as reached to almost 1.6 times (330 N) and the last peak was approaching 500 N for nylon 12, while nylon 6/6 and nylon 11 were 440 N and 456 N respectively.

#### 4.5.3 Result for 4-unit cell of beam thickness 19.05 mm

In this simulation, beam thickness of 19.05 mm was used with same unit cell of four and displacement loading of 15 mm was applied in LS-DYNA.

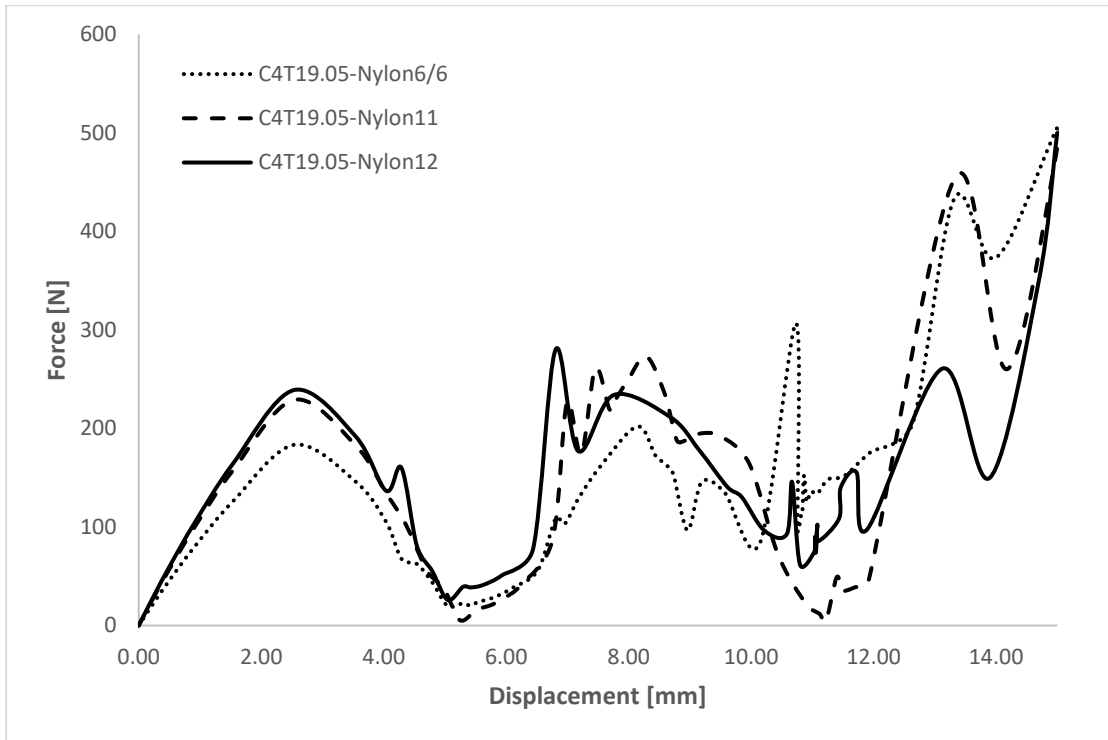


Figure 22. Force-displacement relationship of C4-T19.05 mm on the honeycomb model.

The force threshold of 183 N was noticed for nylon 6/6 material which is 1.2 time less than other two nylon material nylon 11 and 12 (229 and 239 N respectively). For the second loading the force of nylon 12 started ahead of other materials (280 N) at 6.81 mm, while the nylon 6/6 and nylon 11 were increased at almost 8 mm (202 and 273 N respectively). And the forces kept increased to apply the third mode of buckling of the specimen to achieve the negative stiffness behavior and to regain its original shape.

#### 4.5.4 Result for 5-unit cell of beam thickness 6.35 mm

After applying four- unit cell of formed honeycomb, the study of the 5-unit cell model in this section is discussed.

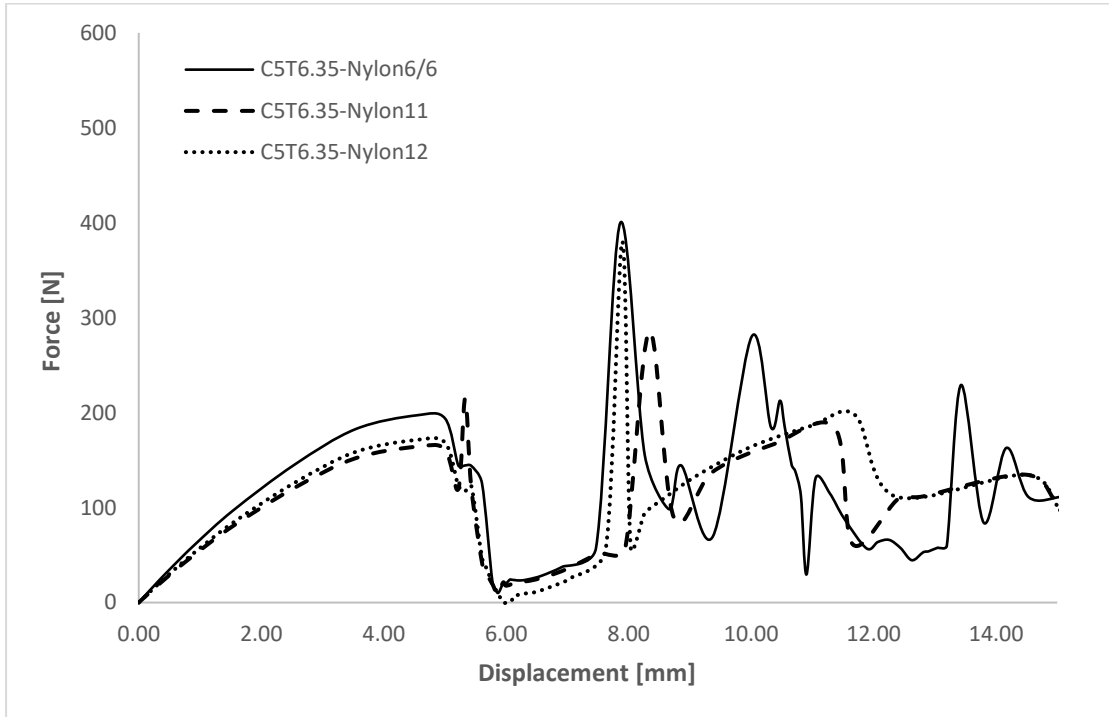


Figure 23. Force-displacement relationship of C5-T6.35 mm on the honeycomb model.

Using a 5-unit cell model of honeycomb, the force threshold during loading for nylon-6/6 (193 N) was the highest among other materials (nylon 11 and 12) as shown in Figure 23. During the second peak, nylon 11 took almost 0.30 mm to reach its peak value (285 N) and then kept fluctuating which showed a negative stiffness behavior. The material nylon-6/6 is not stable in this run might be due to some experimental stress-strain values.

#### 4.5.5 Result for 5-unit cell of beam thickness 19.05 mm

The unit cell of 5-unit cell of honeycomb and a beam thickness of 19.05 mm was discussed considering the three different material type (Nylon 6/6.etc.) and force to displacement loading relationship was examined.

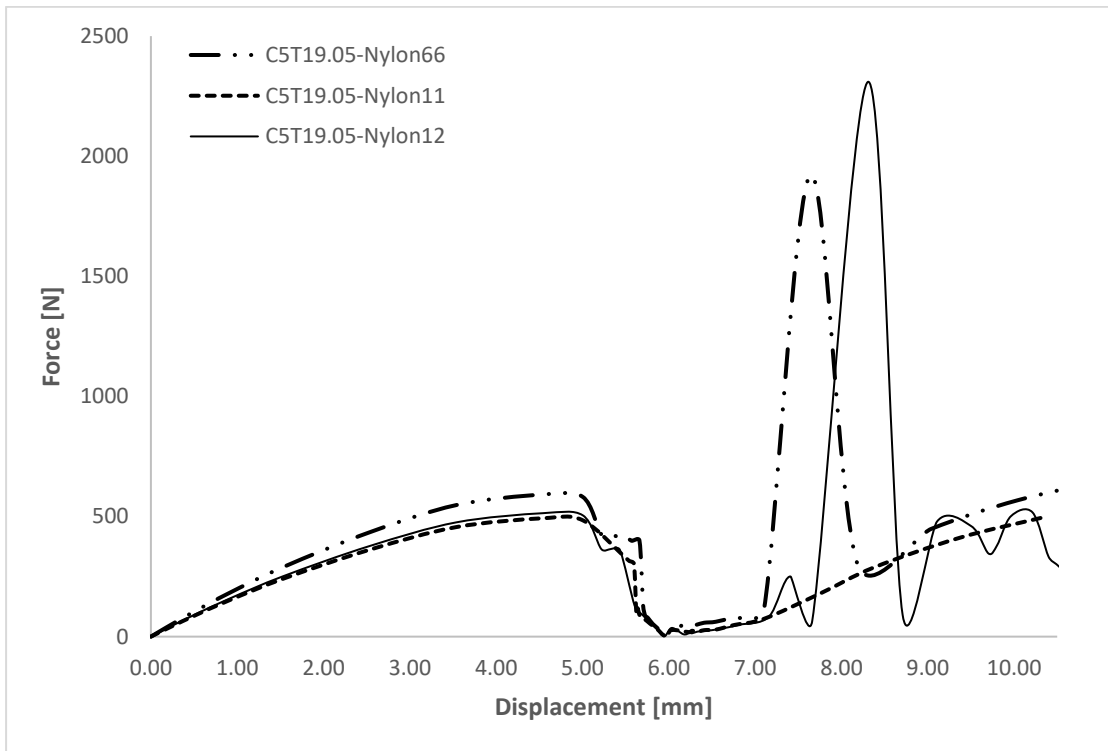


Figure 24. Force-displacement relationship of C5-T19.05 mm on the honeycomb model.

The unit cell of 5 number with three different materials applied in the simulation while the beam thickness is fixed as 19.05 mm. In Figure 24, the force threshold for three materials during the first peak (loading period) was in the range of 500- 515 N. But during the second loading phase the nylon 11 was reached to 400 N as in the second peak less force is required to apply the buckling. Despite that, the force threshold of nylon 12 and nylon 6/6 was approached to almost 2500 N.



#### 4.5.6 Result for 7-unit cell of beam thickness 6.35 mm

seven-unit cell arrangement of honeycomb model as shown in Figure 12 in chapter 3 were used in the FEA run. The beam thickness of 6.35 was applied on the same three assigned materials, then 12.7 mm thickness and last beam thickness of 19.05 mm were applied as to be discussed in the following section. In first part of simulation a beam thickness of 6.35 mm was identified and study on various materials was performed.

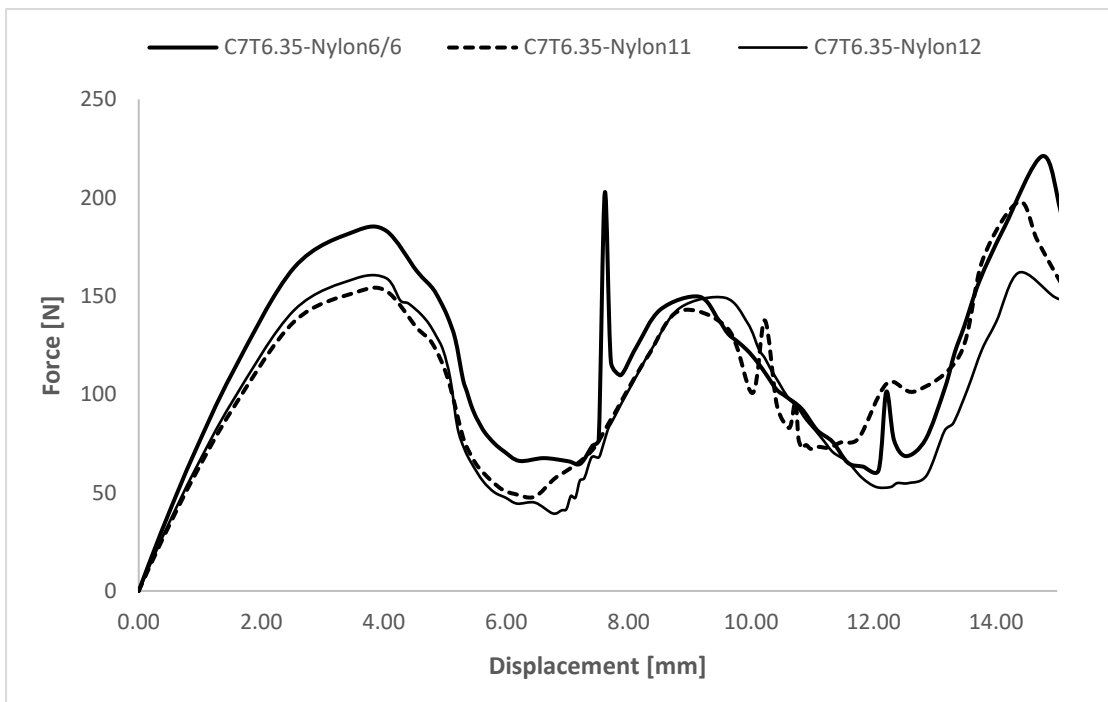


Figure 25. Force-displacement relationship of C7-T6.35 mm on the honeycomb model.

A force threshold of 183 N was displayed in the loading phase for nylon 6/6 material, which was 1.15 times the force of nylon 12. The force values were increased when the displacement reaches to 15 mm and the highest force value was in nylon 6/6 material (approximately 221 N) as shown in Figure 25.

#### 4.5.7 Result for 7-unit cell of beam thickness 12.7 mm

In this modeled honeycomb structure, the unit cell of 7-unit cell of honeycomb and a beam thickness of 12.7 mm was applied in the simulation part in LS-DYNA and the three different material type (Nylon-6/6, etc.) was considered and force to displacement loading relationship was analyzed.

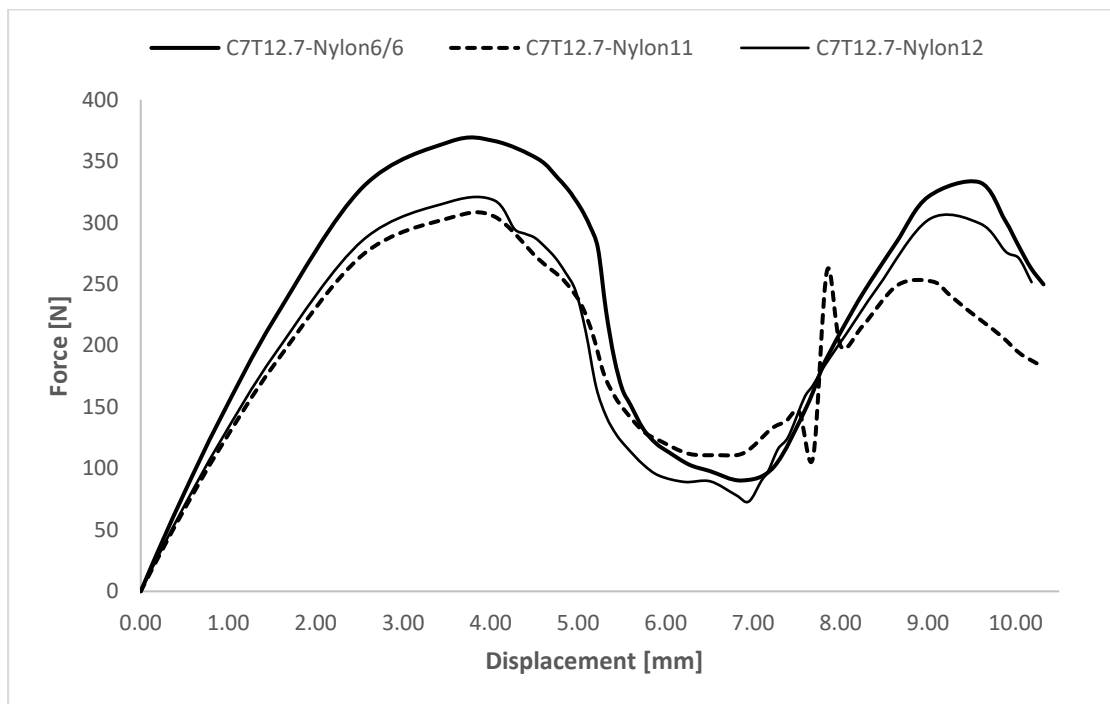


Figure 26. Force-displacement relationship of C7-T12.7 mm on the honeycomb model.

The force threshold in Figure 26 are almost have same value (approximately 300 N) during the loading period (first peak) in both nylon 11 and nylon 12 while it was increased by 23% for nylon 6/6. However, in the second peak nylon 12 and nylon 6/6 were in the same range of force threshold (320 N) and nylon 11 was less by around 22% (250 N).

#### 4.5.8 Result for 7-unit cell of beam thickness 19.05 mm

Finally, Figure 27 shows the force- displacement response of simulation applied in LS-DYNA for honeycomb structure with an arrangement of 7-unit cell and beam thickness of 19.05 mm. the force threshold was achieved the first peak at 4 mm displacement. Force of nylon 6/6 (550 N) was about 1.16 times force in nylon 11 (476 N). the force threshold bounces back for the three different materials studied. After 12 mm of displacement, force of nylon 11 material was not stable as it reaches 716 N at 12.85 and at short time (at 13.8 mm) the force was 908 N. Also, for short period of time the force decreased twice as it was 366 at 14 mm displacement and 337 at 14.66 mm of displacement.

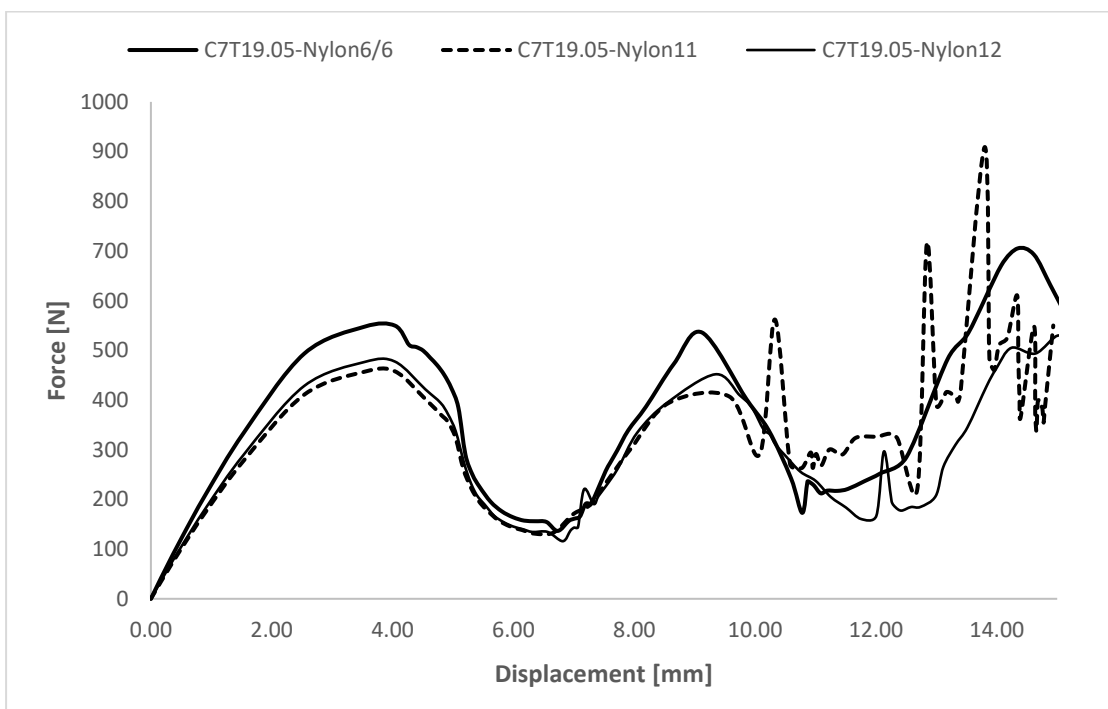


Figure 27. Force-displacement relationship of C7-T19.05 mm on the honeycomb model.

## CHAPTER 5: CONCLUSION AND FUTURE WORK

In summary, the negative stiffness honeycomb behaves very similarly to conventional honeycombs, with a linear stiffness at first under compression loading. It is the recovery of the original shape and dimensions of the honeycombs that makes them attractive; despite going through compression to the point of densification, they retain their original shape and dimensions.

The thesis meticulously studied the mechanical performance of multiple models of honeycomb structure with applying negative stiffness behavior on the models by using FEA runs in LS-DYNA, the quasi-static displacement loading was applied and the force threshold of the each NSH structures were explored. A model of NSH structure was developed and simulated in FEA for validation. The force threshold during loading and unloading phase in validation part for the applied honeycomb model was 289 N, while the referenced paper force values was 275 N which indicates an error of 5 %. After the model was validated, it was used to study the effect of changing three different parameters on the modeled honeycomb structure.

First, the effect of material change was studied by applying nylon 11, nylon 12 and nylon 6/6 as different material and evaluate the force threshold at beam thickness of 12.70 mm and 5-unit cell model of honeycomb structure and the result shows that the nylon 11 material is the best option compared to other studied material as the force threshold was the lowest with value of 328 N while the nylon 12 and 6/6 were 342 N and 394 N. Accordingly, the nylon 11 used as material for honeycomb structure since it shows good contribution in decreasing the force threshold due to its materials properties to maintain the stability of the model and helps regain its original shape which confirms the achievement of negative stiffness behavior on the model.

Then, three different beam thickness of 6.35 mm, 12.70 mm and 19.05 mm was modeled, and three runs were simulated in LS-Dyna for each beam thickness considering nylon 11 as material. The force threshold value of 492 N was required for the beam thickness of 19.05 mm during the first loading and unloading phase. And force 164 N was noticed for the beam thickness of 6.35 mm. Results indicate that force threshold capacities of the models increase with increasing thickness values intervals.

Also, the force threshold was investigated for applying multiple numbers of unit cell on the honeycomb structure. Four-, five- and seven-unit cell numbers were modeled in this study in LS-Dyna to investigate their effect on the force threshold. For 4-unit cell number model, the force obtained was 152 N at displacement of 2.54 mm, force values of 241 N and 274 N for 5- and 7- unit cell arrangement were observed respectively at 2.54 mm of displacement loading. Results concludes that the unit cell numbers with its arrangement have a significant role in determining the compressive force characteristics of NSH structures.

Finally, the parametric study was examined for various models of the validated honeycomb structure, and conclusion derived as follows:

- For 4- unit cell number model:
  - Three materials of nylon 6/6, 11 and 12 for beam thickness of 6.35 mm was simulated. The highest force threshold was found in nylon 6/6 material with values of 100 N, 620 N, 193 N and 700 N during first, second, third and fourth peak in loading and unloading phase. The nylon 6/6 material was the highest achieved force values since the yield strength applied was 1900 MPa that is the highest value compared to other materials (nylon 11 and 12) which requires additional force to achieve negative stiffness behavior.

- Then, for beam thickness of 12.7 mm the force threshold for the first phase was 152 N, 160 N and 183 N for nylon 11, 12 and 6/6 respectively.
  - The force threshold values obtained for the beam thickness of 19.05 mm were 183 N, 229 N, 239 N for nylon 6/6, 11 and 12 respectively.
  - This concludes that with the increase of beam thickness of the honeycomb structure, the force increases as it requires more force to reach to buckled beam behavior.
- For 5- unit cell number model:
  - The force value of 197 N was noted for the nylon 6/6 material at beam thickness of 6.35- mm, while forces of nylon 12 and nylon 11 were noted to be 171 N and 164 N respectively at displacement value of 4.54 mm.
  - At beam thickness of 19.05 mm, at the first peak of loading and unloading phase, the force threshold was almost 500 N for all materials applied in this simulation. During the second peak, the force needed to buckle the model increases dramatically (above 100 N) for nylon 6/6 and nylon 12 while for nylon 11 the force threshold was within range of 400-450 N.
  - The material properties have major influence on the force threshold that shall be kept in reasonable range to reach to the buckling mode of the honeycomb structure. Also, the force threshold increases proportionally with the increase of unit cell numbers applied in the honeycomb structures.
- For 7- unit cell number model:

The force threshold increases with the increase of beam thickness of the modeled honeycomb structure, the lowest force threshold values was achieved for nylon 11

material with the increase of beam thickness from 6.35 mm to 19.05 mm. For nylon 11, the force values were 152 N, 305 N and 477 N for beam thickness of 6.35 mm, 12.7 mm, and 19.05 mm respectively during loading and unloading phase.

Overall, a honeycomb structure tends to give a greater force response with more unit cells of honeycomb structure and with increase in beam thickness. And from material perspective applied on the honeycomb model, the material properties of the material applied has major role on the force threshold required to achieve the negative stiffness behavior for the honeycomb structure.

A honeycomb with negative stiffness can be used as an impact protection device such as bumper, a helmet and bicycle seat. In addition to their energy absorbing capabilities, honeycombs are also completely reversible, making them an ideal material for creating long-lasting impact protections. Likewise, suspension systems could benefit from negative stiffness behavior to protect occupants from impacts exceeding the injury limit.

Following points were addressed to support the findings in this thesis and might be investigated in future studies:

- Dynamic investigation for the negative stiffness honeycomb structure is recommended by considering the mass of each model.
- Different parameters like materials, apex height and honeycomb shell thickness can be changed and investigated in both quasi static and dynamic analysis.
- Energy absorption can be further investigated using all models used in the parametric study applied in this thesis.

- Reusable packaging can be developed based on the recoverability of honeycombs, thereby allowing the package's contents to withstand repeated impacts.
- Applying LS topology optimization tool on the designed model which helps to compute optimal designs according to specified constraints to achieve minimal resources without any wastage in the production phase. Case study is attached in the appendix section.



## REFERENCES

- [1] K. Marsh and B. Bugusu, “Food packaging - Roles, materials, and environmental issues: Scientific status summary,” *Journal of Food Science*, vol. 72, no. 3, 2007. doi: 10.1111/j.1750-3841.2007.00301.x.
- [2] D. A. Debeau, C. C. Seepersad, and M. R. Haberman, “Impact behavior of negative stiffness honeycomb materials,” *J Mater Res*, vol. 33, no. 3, pp. 290–299, 2018, doi: 10.1557/jmr.2018.7.
- [3] D. Pietrosanti, M. de Angelis, and M. Basili, “A generalized 2-DOF model for optimal design of MDOF structures controlled by Tuned Mass Damper Inerter (TMDI),” *Int J Mech Sci*, vol. 185, 2020, doi: 10.1016/j.ijmecsci.2020.105849.
- [4] Z. P. Bazant, L. Cedolin, and M. R. Tabbara, “New method of analysis for slender columns,” *ACI Struct J*, vol. 88, no. 4, 1991, doi: 10.14359/2679.
- [5] X. Wang, T. He, Y. Shen, Y. Shan, and X. Liu, “Parameters optimization and performance evaluation for the novel inerter-based dynamic vibration absorbers with negative stiffness,” *J Sound Vib*, vol. 463, 2019, doi: 10.1016/j.jsv.2019.114941.
- [6] A. Batou and S. Adhikari, “Optimal parameters of viscoelastic tuned-mass dampers,” *J Sound Vib*, vol. 445, 2019, doi: 10.1016/j.jsv.2019.01.010.
- [7] J. Qiu, J. H. Lang, and A. H. Slocum, “A curved-beam bistable mechanism,” *Journal of Microelectromechanical Systems*, vol. 13, no. 2, pp. 137–146, 2004, doi: 10.1109/JMEMS.2004.825308.
- [8] B. A. Fulcher, D. W. Shahan, M. R. Haberman, C. C. Seepersad, and P. S. Wilson, “Analytical and experimental investigation of buckled beams

- as negative stiffness elements for passive vibration and shock isolation systems,” *Journal of Vibration and Acoustics, Transactions of the ASME*, vol. 136, no. 3, pp. 1–12, 2014, doi: 10.1115/1.4026888.
- [9] T. Klatt, M. Haberman, and C. C. Seepersad, “Selective laser sintering of negative stiffness mesostructures for recoverable, nearly-ideal shock isolation,” in *24th International SFF Symposium - An Additive Manufacturing Conference, SFF 2013*, 2013.
- [10] L. Kashdan, C. C. Seepersad, M. Haberman, and P. S. Wilson, “Design, fabrication, and evaluation of negative stiffness elements using SLS,” *Rapid Prototyp J*, vol. 18, no. 3, pp. 194–200, 2012, doi: 10.1108/13552541211218108.
- [11] B. A. Fulcher, D. W. Shahan, M. R. Haberman, C. C. Seepersad, and P. S. Wilson, “Analytical and experimental investigation of buckled beams as negative stiffness elements for passive vibration and shock isolation systems,” *Journal of Vibration and Acoustics, Transactions of the ASME*, vol. 136, no. 3, pp. 1–12, 2014, doi: 10.1115/1.4026888.
- [12] D. M. Correa, T. Klatt, S. Cortes, M. Haberman, D. Kovar, and C. Seepersad, “Negative stiffness honeycombs for recoverable shock isolation,” *Rapid Prototyp J*, vol. 21, no. 2, 2015, doi: 10.1108/RPJ-12-2014-0182.
- [13] A. Rafsanjani, A. Akbarzadeh, and D. Pasini, “Snapping Mechanical Metamaterials under Tension,” *Advanced Materials*, vol. 27, no. 39, pp. 5931–5935, 2015, doi: 10.1002/adma.201502809.
- [14] X. Tan, B. Wang, S. Chen, S. Zhu, and Y. Sun, “A novel cylindrical negative stiffness structure for shock isolation,” *Compos Struct*, vol. 214,

pp. 397–405, 2019, doi: 10.1016/j.compstruct.2019.02.030.

- [15] S. Cortes, J. Allison, C. Morris, M. R. Haberman, C. C. Seepersad, and D. Kovar, “Design, Manufacture, and Quasi-Static Testing of Metallic Negative Stiffness Structures within a Polymer Matrix,” *Exp Mech*, vol. 57, no. 8, pp. 1183–1191, 2017, doi: 10.1007/s11340-017-0290-2.
- [16] C. S. Ha, R. S. Lakes, and M. E. Plesha, “Design, fabrication, and analysis of lattice exhibiting energy absorption via snap-through behavior,” *Mater Des*, vol. 141, pp. 426–437, 2018, doi: 10.1016/j.matdes.2017.12.050.
- [17] D. M. Correa, T. D. Klatt, S. A. Cortes, M. R. Haberman, D. Kovar, and C. C. Seepersad, “Negative stiffness honeycombs for recoverable shock isolation,” in *25th Annual International Solid Freeform Fabrication Symposium &#65533; An Additive Manufacturing Conference, SFF 2014*, 2014.
- [18] T. A. M. Hewage, K. L. Alderson, A. Alderson, and F. Scarpa, “Double-Negative Mechanical Metamaterials Displaying Simultaneous Negative Stiffness and Negative Poisson’s Ratio Properties,” *Advanced Materials*, vol. 28, no. 46, pp. 10323–10332, 2016, doi: 10.1002/adma.201603959.
- [19] J. Meaud and K. Che, “Tuning elastic wave propagation in multistable architected materials,” *Int J Solids Struct*, vol. 122–123, pp. 69–80, 2017, doi: 10.1016/j.ijsolstr.2017.05.042.
- [20] E. B. Duoss *et al.*, “Three-dimensional printing of elastomeric, cellular architectures with negative stiffness,” *Adv Funct Mater*, vol. 24, no. 31, pp. 4905–4913, 2014, doi: 10.1002/adfm.201400451.
- [21] S. Chen *et al.*, “A novel composite negative stiffness structure for recoverable trapping energy,” *Compos Part A Appl Sci Manuf*, vol. 129,

2020, doi: 10.1016/j.compositesa.2019.105697.

- [22] X. Tan *et al.*, “Mechanical response of negative stiffness truncated-conical shell systems: experiment, numerical simulation and empirical model,” *Compos B Eng*, vol. 188, 2020, doi: 10.1016/j.compositesb.2020.107898.
- [23] M. M. Osman, M. Shazly, E. A. El-Danaf, P. Jamshidi, and M. M. Attallah, “Compressive behavior of stretched and composite microlattice metamaterial for energy absorption applications,” *Compos B Eng*, vol. 184, 2020, doi: 10.1016/j.compositesb.2019.107715.
- [24] T. Frenzel, C. Findeisen, M. Kadic, P. Gumbsch, and M. Wegener, “Tailored Buckling Microlattices as Reusable Light-Weight Shock Absorbers,” *Advanced Materials*, vol. 28, no. 28, pp. 5865–5870, 2016, doi: 10.1002/adma.201600610.
- [25] N. S. Ha and G. Lu, “A review of recent research on bio-inspired structures and materials for energy absorption applications,” *Composites Part B: Engineering*, vol. 181, 2020, doi: 10.1016/j.compositesb.2019.107496.
- [26] L. N. Virgin and R. B. Davis, “Vibration isolation using buckled struts,” *J Sound Vib*, vol. 260, no. 5, pp. 965–973, 2003, doi: 10.1016/S0022-460X(02)01177-X.
- [27] C. M. Lee, V. N. Goverdovskiy, and A. I. Temnikov, “Design of springs with ‘negative’ stiffness to improve vehicle driver vibration isolation,” *J Sound Vib*, vol. 302, no. 4–5, 2007, doi: 10.1016/j.jsv.2006.12.024.
- [28] T. D. Le and K. K. Ahn, “Experimental investigation of a vibration isolation system using negative stiffness structure,” *Int J Mech Sci*, vol.

70, pp. 99–112, 2013, doi: 10.1016/j.ijmecsci.2013.02.009.

- [29] X. Huang, X. Liu, J. Sun, Z. Zhang, and H. Hua, “Vibration isolation characteristics of a nonlinear isolator using euler buckled beam as negative stiffness corrector: A theoretical and experimental study,” *J Sound Vib*, vol. 333, no. 4, pp. 1132–1148, 2014, doi: 10.1016/j.jsv.2013.10.026.
- [30] W. Wu, X. Chen, and Y. Shan, “Analysis and experiment of a vibration isolator using a novel magnetic spring with negative stiffness,” *J Sound Vib*, vol. 333, no. 13, pp. 2958–2970, 2014, doi: 10.1016/j.jsv.2014.02.009.
- [31] D. L. Platus, “Negative-stiffness-mechanism vibration isolation systems,” in *Vibration Control in Microelectronics, Optics, and Metrology*, 1999, vol. 1619. doi: 10.1117/12.56823.
- [32] W. Roux, “LS-TaSCTM- TOPOLOGY AND SHAPE COMPUTATIONS FOR LS-DYNA User’s Manual,” *Livermore Software Technology Corporation*, Livermore, 2011.

## APPENDIX I: LS-DYNA SIMULATION MODELS

In this appendix, all models applied in LS-DYNA software for parametric study section are attached. First, model of 4-unit cell with beam thickness of 6.35 mm, 12.7 mm and 19.05 mm are formed with assigning three different materials for each of the beam thickness run for the specific unit cell arrangement as shown in Figure 28 (a), (b) and (c) respectively. Then, unit cell of five numbers with the same sequence are modeled as illustrated in Figure 29 (a), (b) and (c). Finally, Figure 30 (a), (b) and (c) present 7-unit cell model of honeycomb structure in the finite element analysis with the same pattern of beam thickness and same three materials (nylon 11, 6/6 and 12).

All models as attached in the following figures are collected from LS-DYNA software.

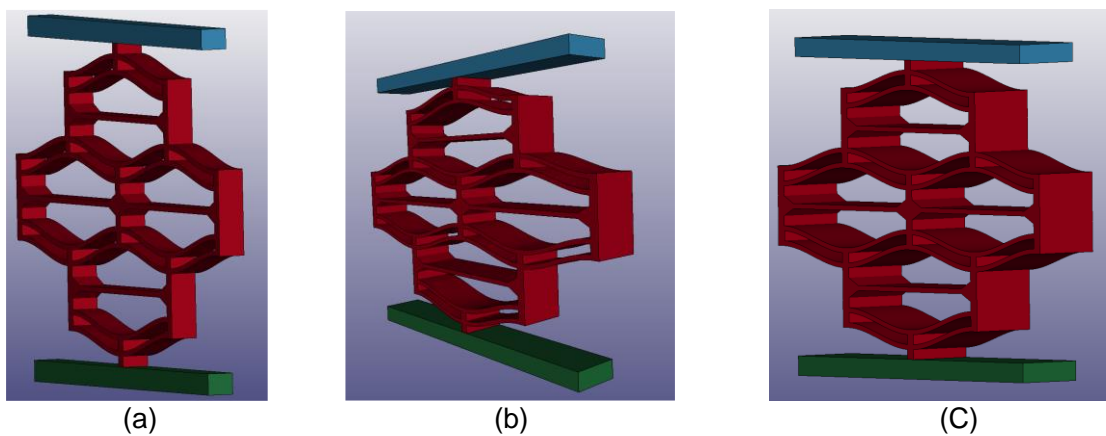


Figure 28. FEA model of the 4-unit cell (a) beam thickness of 6.35 mm (b) beam thickness of 12.7 mm (c) beam thickness of 19.05 mm

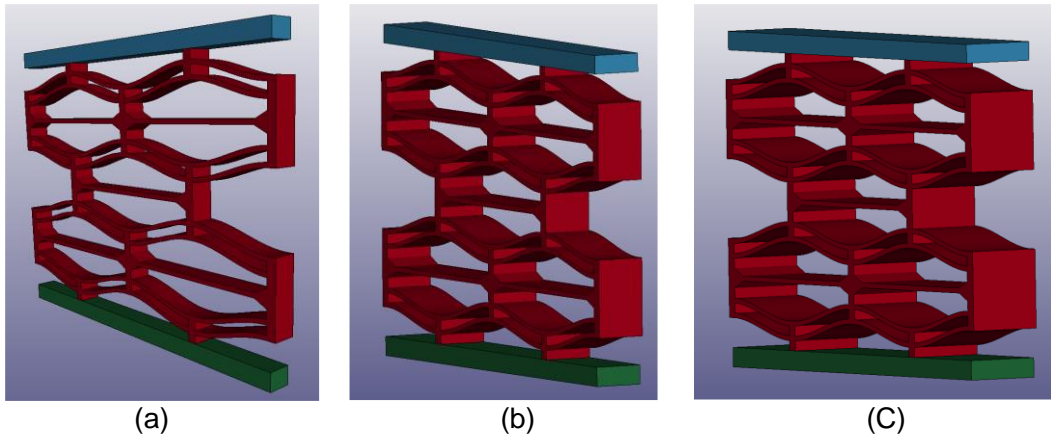


Figure 29. FEA model of the 5-unit cell (a) beam thickness of 6.35 mm (b) beam thickness of 12.7 mm (c) beam thickness of 19.05 mm

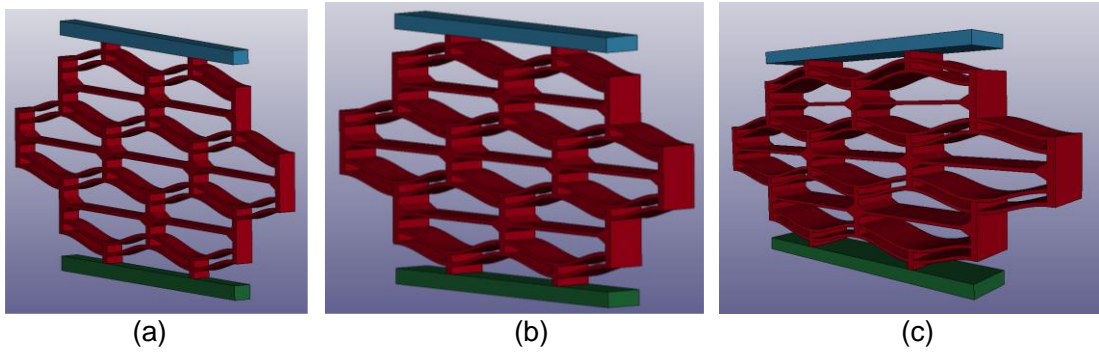


Figure 30. FEA model of the 7-unit cell (a) beam thickness of 6.35 mm (b) beam thickness of 12.7 mm (c) beam thickness of 19.05 mm

## APPENDIX II: CASE STUDY LS-TOPOLOGY OPTIMIZATION TOOL

In this appendix, case study for ls topology optimization tool is discussed. The case study contributes to the topology optimization tool of structures under non-linear dynamic loading. The software tool called LS-TaSC which was named LS-topology/OPT in the first version released. This tool can be implemented to nonlinear static and dynamic problems. The method used in this tool named as hybrid cellular Automata (HCA) which is free of gradient and heuristic approach and the objective is to accomplish structure with uniformly internal energy density subject to given mass fraction. Figure 31 envisions the HCA algorithm applied in topology optimization, the design variables in each finite element are the relative density, young modulus, hardening parameter, and yield stress). The relative density is adapted, and the process starts for convergence as it keeps updating till convergence criterion is met.

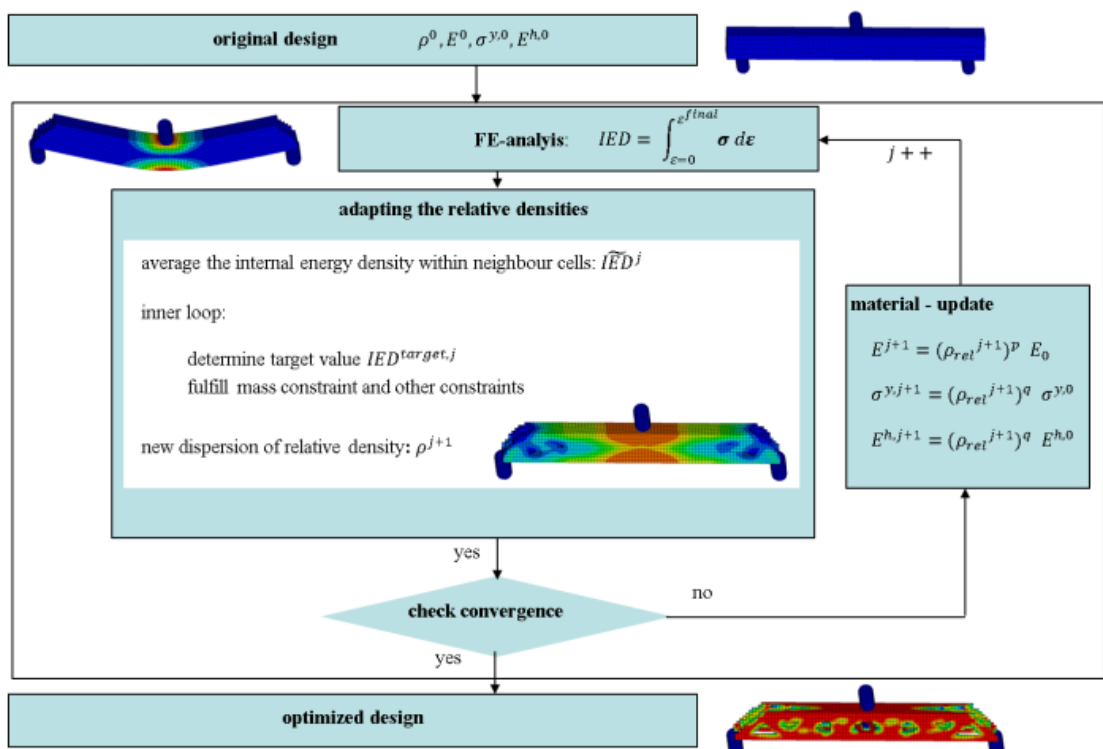


Figure 31 HCA algorithm- LS topology optimization [32]



The application of a knee bumper was demonstrated in this case study by applying HCA method as illustrated in figure 31. The knee bumper as shown in figure 32 before optimization was modeled. the height of knee bumper was 120 mm supported, the material assigned was aluminum with density of  $2.7 \text{ E}^{-09}$  , young's modulus (E) of  $70\text{E}^{+03} \text{ N/mm}^2$  , poisson's ratio of 0.33 and yield strength of  $240 \text{ N/mm}^2$ . While the rigid impactor was given with mass of (0.27 t) and initial velocity of (1250 mm/s).

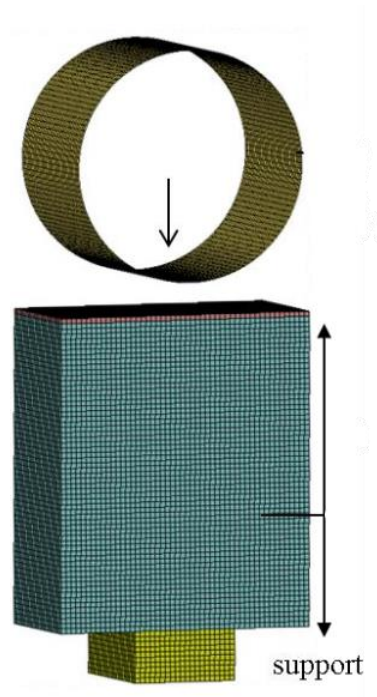


Figure 32 Knee bumper application

Table 6 optimization input for the topology (HCA) method

<b>Design variables</b>	In every finite element, relative density
<b>Objective is fixed</b>	homogenization of the internal energy density
<b>Constraints is fixed</b>	<u>Mass constraint:</u> relative mass $M^{\text{rel}} \leq 0.2$ is prescribed. <u>Displacement constraint:</u> impactor penetration $d_{\text{max}} \leq 2\text{mm}$

So, the optimization input for the topology method is listed in table 6 and the HCA method used tends to enforce a fully stress design.

Results- optimized topology:

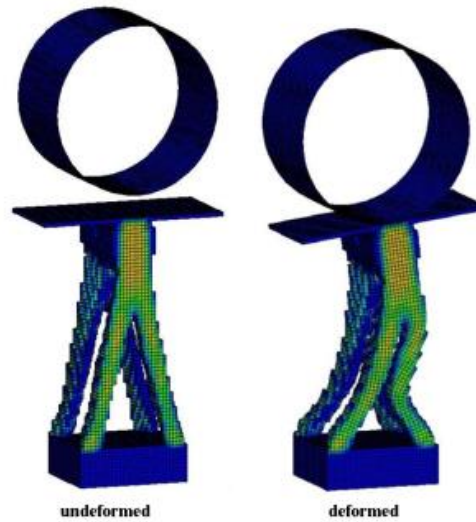


Figure 33 Optimized design of the knee bumper

The HCA method applied converges to a feasible topology, The transfer of the impacting load to the ground makes sense for the optimized structures for the undeformed and deformed model as illustrated in figure 33.

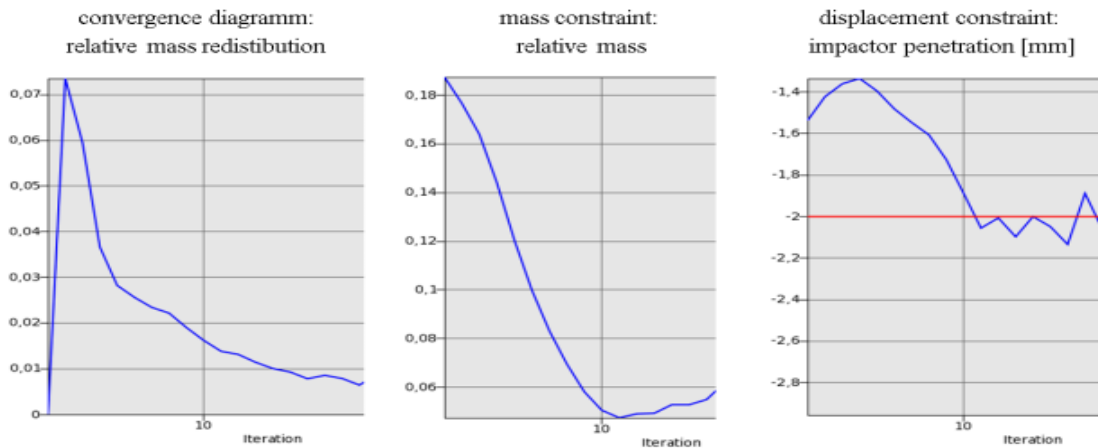


Figure 34 Convergence diagram, displacement and mass constraints for the optimized topology method (HCA)

Based on table 6 optimization input, The relative mass constraint was less than or equal to 0.2 and max displacement constraint of less than or equal 2 mm are achieved for the hybrid cellular Automata method and convergence is achieved within 18 analyses in LS-DYNA software (18 iterations) as shown in graphs in figure 34.

This case study concludes that topology optimization is a method that optimizes the layout of materials in given design space while considering the loads, boundary conditions and constraints to enhance system performance.